THE JOURNAL OF BIOLOGICAL CHEMISTRY VOL. 284, NO. 6, pp. 3396–3407, February 6, 2009

Linkage between Phosphorylation of the Origin Recognition Complex and Its ATP Binding Activity in *Saccharomyces cerevisiae*[*S]

Received for publication, June 4, 2008, and in revised form, December 3, 2008 Published, JBC Papers in Press, December 8, 2008, DOI 10.1074/jbc.M804293200

Masaki Makise, Masaya Takehara, Akihiko Kuniyasu, Nanako Matsui, Hitoshi Nakayama, and Tohru Mizushima[1]

From the Graduate School of Medical and Pharmaceutical Sciences, Kumamoto University, Kumamoto 862-0973, Japan

The initiation of chromosomal DNA replication is tightly regulated to achieve genome replication just once per cell cycle and cyclin-dependent kinase (CDK) plays an important role in this process. Adenine nucleotides that bind to the origin recognition complex (ORC) are also suggested to be involved in this process. Of the six subunits of the *Saccharomyces cerevisiae* ORC (Orc1–6p), both Orc1p and Orc5p have ATP binding activity, and both Orc2p and Orc6p are phosphorylated by CDK in cells. In this study we constructed a series of yeast strains expressing phospho-mimetic mutants of Orc2p or Orc6p and found that expression of a Ser-188 mutant of Orc2p (Orc2-5Dp) delays G_1-S transition and S phase progression and causes the accumulation of cells with 2C DNA content. Using antibody that specifically recognizes Ser-188-phosphorylated Orc2p, we showed that Ser-188 is phosphorylated by CDK in a cell cycle-regulated manner. Expression of Orc2-5Dp caused phosphorylation of Rad53p and inefficient loading of the six minichromosome maintenance proteins. These results suggest that the accumulation of cells with 2C DNA content is due to inefficient origin firing and induction of the cell cycle checkpoint response and that dephosphorylation of Ser-188 of Orc2p in late M or G_1 phase may be involved in pre-RC formation. *In vitro*, a purified mutant ORC containing Orc2-5Dp lost Orc5p ATP binding activity. This is the first demonstration of a link between phosphorylation of the ORC and its ability to bind ATP, which may be important for the cell cycle-regulated initiation of DNA replication.

The initiation of chromosomal DNA replication is tightly regulated to replicate the genome just once per cell cycle. To achieve this, both induction of initiation at the G_1-S boundary and inhibition of initiation in other phases of the cell cycle are required. The mechanisms governing this regulation in eukaryotes have been studied the most extensively in budding yeast (*Saccharomyces cerevisiae*), and we describe mostly events in budding yeast in this paper otherwise noticed. Cyclin-dependent protein kinases (CDKs)[2] play essential roles in both the induction and inhibition of initiation; low CDK activity in late M and G_1 phases is required to prepare for initiation of DNA replication, and high CDK activity in S, G_2, and early M phases is required for suppression of re-initiation of DNA replication before cell division. This high CDK activity is also involved in initiation of DNA replication at the G_1-S boundary (1–4).

Cell cycle-regulated formation of protein complexes on origins of chromosomal DNA replication is a key step in regulation of the initiation of DNA replication. In G_1 phase (under low CDK activity), a protein complex called the "pre-replication complex (pre-RC)" is formed on each origin. The pre-RC contains several proteins including the origin recognition complex (ORC), Cdc6p, Cdt1p, and the six minichromosome maintenance proteins (MCM), Mcm2–7p. The ORC was originally identified as a six-protein complex that specifically bound to *S. cerevisiae* origins of DNA replication (5), and its homologues have been found in various eukaryotic species, including human (3). In this manuscript, "ORC" refers to *S. cerevisiae* ORC. The ORC is bound to chromatin at the origins of chromosomal DNA replication throughout the cell cycle and is thought to function as a "landing pad" for the assembly of pre-RC. At the G_1-S boundary, CDK and another kinase (Cdc7p-Dbf4p) activate the pre-RC to initiate chromosomal DNA replication. After initiation, re-formation of the pre-RC is strictly prohibited to suppress re-initiation of DNA replication, and high CDK activity is essential for this process; artificial inhibition of CDK activity in G_2 phase resulted in re-formation of pre-RC and re-initiation of DNA replication (6–8). The B type cyclin-CDK complex affects initiation of DNA replication through two distinct mechanisms, phosphorylation of, or direct binding to replication-related proteins (9, 10). Therefore, identification of the components of the protein complex present on origin DNA that are phosphorylated by CDK and an understanding of the role of this phosphorylation are important for understanding the mechanisms which ensure that replication occurs just once per cell cycle.

It has been suggested that Orc2p, Orc6p, Cdc6p, and MCM are phosphorylated by CDK in a cell cycle-regulated manner.

* This work was supported by grants-in-aid for Scientific Research from the Ministry of Education, Culture, Sports, Science, and Technology, Japan. The costs of publication of this article were defrayed in part by the payment of page charges. This article must therefore be hereby marked "*advertisement*" in accordance with 18 U.S.C. Section 1734 solely to indicate this fact.

[S] The on-line version of this article (available at http://www.jbc.org) contains supplemental Fig. S1.

[1] To whom correspondence should be addressed: 5-1 Oe-honmachi, Kumamoto 862-0973, Japan. Tel. and Fax: 81-96-371-4323; E-mail: mizu@gpo.kumamoto-u.ac.jp.

[2] The abbreviations used are: CDK, cyclin-dependent protein kinase; ORC, origin recognition complex; pre-RC, pre-replicative complex; MCM, minichromosome maintenance proteins; 5-FOA, 5-fluoroorotic acid; HA, hemagglutinin; α-factor, α-mating factor; ChIP, chromatin immunoprecipitation; *ARS1*, autonomously replicating sequence 1; GST, glutathione *S*-transferase; FACS, fluorescence-activated cell sorter.

Phosphorylation of Cdc6p or MCM seems to cause its degradation or nuclear exclusion, respectively (11–17). Furthermore, the expression of degradation-resistant Cdc6p and Mcm7p with an exogenous nuclear localization signal with the expression of mutant forms of Orc2p and Orc6p in which possible CDK-phosphorylated sites are mutated to be inert, induced re-formation of the pre-RC and re-initiation of DNA replication without inhibition of CDK (18, 19). These results suggest that CDK-dependent phosphorylation of ORC, Cdc6p, and MCM play an important role in suppression of re-formation of pre-RC and re-initiation of DNA replication. However, at present it is unclear which subunit (Orc2p or Orc6p) or which possible CDK-phosphorylated site is responsible for this regulation and how the phosphorylation of ORC suppresses the re-initiation of DNA replication. Furthermore, the role of dephosphorylation of ORC in late M or G_1 phase cannot be ruled out by use of mutants that are inert for phosphorylation. To address these issues, characterization of phospho-mimetic mutants (in which particular CDK target amino acid residues are substituted with Asp or Glu) is useful. For example, analysis of a phospho-mimetic mutant of Sld2p suggested that phosphorylation of Sld2p is responsible for CDK-dependent initiation of DNA replication (20–22).

As is the case for the bacterial initiator of chromosomal DNA replication, DnaA (23–27), adenine nucleotides bound to the ORC seem to regulate the initiation of DNA replication. The ORC has two subunits (Orc1p and Orc5p), which bind ATP (28, 29). Orc1p, but not Orc5p, has ATPase activity, which stimulates the loading of MCM onto origins (30, 31). Orc5p, but not Orc1p, can bind ADP (32). The binding of ATP to Orc1p, but not to Orc5p, is essential for the specific binding of ORC to origin DNA (28, 29). ATP binding to Orc5p increases the affinity of Orc1p for ATP *in vitro* (29) and is important for maintaining the stability of ORC *in vivo* (33, 34). However, a link between phosphorylation of ORC and its ATP binding activity has not been previously established.

In this study we constructed a series of yeast strains expressing phospho-mimetic mutant Orc2p or Orc6p for each possible CDK-phosphorylated site. We found that expression of a Ser-188 mutant of Orc2p, but not of other CDK-phosphorylated site mutants, delays cell growth, G_1-S transition, S phase progression, and pre-RC formation. This suggests that Ser-188 is the key amino acid residue in CDK-dependent regulation of ORC. Thus, dephosphorylation of Ser-188 of Orc2p in late M or G_1 phase may be involved in the formation of pre-RC. *In vitro*, the purified phospho-mimetic mutant ORC containing the Ser-188 Orc2p mutant retained the ATP binding activity of Orc1p and origin DNA binding activity but lost the ATP binding activity of Orc5p. We consider that phosphorylation of Ser-188 of Orc2p affects pre-RC formation by inhibiting the binding of ATP to Orc5p.

EXPERIMENTAL PROCEDURES

Chemicals, Plasmids, and Strains—[α-^{32}P]ATP (3000 Ci/mmol), [γ-^{32}P]ATP (6000 Ci/mmol), and poly(dI/dC) were purchased from GE Healthcare, and 8-N_3-[γ-^{32}P]ATP was from ALT Bioscience. DNA fragments (290 bp) containing wild-type *ARS1* and mutant *ars1/A⁻B1⁻* were prepared by PCR as described previously (35) and purified by polyacrylamide gel electrophoresis. DNA fragments were radiolabeled by T4 polynucleotide kinase and [γ-^{32}P]ATP as described previously (29). The specific activity of each probe was ~4000 cpm/fmol DNA. Mouse monoclonal antibodies against Orc3p, Mcm2p, and hemagglutinin (HA) were gifts from Dr. Stillman (Cold Spring Harbor Laboratory). Mouse monoclonal antibody against FLAG was purchased from Sigma. Plasmids, pRS403, 405, 413, 416, and 425 were purchased from Invitrogen.

Plasmids pRS413-*ORC2* and pRS416-*ORC2* contain *ORC2* (from −805 to +1909) ligated into the SacI-SalI site. To express HA-tagged Orc2p in cells, pRS413–3HA and pRS413-*GAL1*-3HA were first constructed. Plasmid pRS413–3HA has a triple HA epitope gene (3HA) in the XhoI-ApaI site, and pRS413-*GAL1*-3HA has the *GAL1* promoter (from −457 to −1) in the BamHI-EcoRV site. An expression plasmid, pRS413-*ORC2*-3HA (or pRS413-*GAL1-ORC2*-3HA), contains *ORC2* ligated in-frame with 3HA. A plasmid pRS425-*GAL1-ORC2*-3HA was constructed by insertion of the BssHII-BssHII DNA fragment of pRS413-*GAL1-ORC2*-3HA into the same restriction enzyme site on pRS425. Plasmids pRS413-*ORC6* and pRS416-*ORC6* contain *ORC6* (from −600 to +1808) cloned into the XbaI-XhoI site. Site-directed mutagenesis of the CDK consensus sites was done as described previously (36). DNA fragments containing *orc2- (or orc6)-All-A* were PCR-amplified using chromosomal DNA prepared from pJL1095 and pJL1096 cells (gifts from Dr. Li (University of California, San Francisco)) (18) as templates. A series of expression plasmids for mutant forms of *orc* were constructed by replacement of the wild-type *ORC* gene with each mutant *orc* gene.

S. cerevisiae strains are listed in Table 1 (37, 38). These strains were cultured in YP medium (2% bactopeptone, 1% yeast extract, 2 mg/ml adenine hemisulfate) or synthetic complete medium containing glucose or galactose.

To disrupt the chromosomal *ORC2* or *ORC6*, *TRP1* was inserted between flanking sequences (40 bp) of the *ORC2* or *ORC6*, and this DNA fragment was introduced into the DK186 diploid (resultant strains were YMM10 or YMM18, respectively). We confirmed that all tetrads showed only two viable spores. For plasmid shuffling, plasmid pRS413 (a low copy number plasmid containing *HIS*) (39) with each mutant *orc2* or *orc6* gene, was transformed into YMM10 or YMM18 cells by the lithium acetate method. The transformants were cultured on synthetic complete agar plates containing 2% glucose and 0.1% 5-fluoroorotic acid (5-FOA) at 30 °C for 3 days.

YMM77 is a derivative of YMM10 in which pRS405-*GAL1-orc2-1–3FLAG* was integrated into the *leu2* locus. YMM84 and YMM76 are derivatives of YMM77 in which pRS403-*ORC2*-3HA and pRS403-*orc2-5d*-3HA, respectively, were integrated into the *his3* locus. We confirmed these integrations by PCR and Southern blot analysis.

Preparation of Antibodies and ORC—Rabbit polyclonal antibody against Ser-188-phosphorylated Orc2p (α-Ser(P)-188) was generated against synthetic peptide with the following sequence: NHDFTS(PO_4)PLKQIIC (40). The antibody was purified on a protein A-Sepharose column followed by Sulfolink Coupling Gel (Pierce) coupled with the synthetic peptide. The specificity of the antibody was tested by enzyme-linked

TABLE 1
Yeast strains used in this study

Strains	Genotype	References
W303-1A	*MATa leu2-3,112 ura3-52 can1-100 ade2-1 his3-11 trp1-1*	Ref. 37
DK186	W303-1A *bar1Δ*	Ref. 57
YMM10	DK186 *orc2D::TRP1*[pRS416-*ORC2*]	This study
YMM10-2	YMM10[pRS413]	This study
YMM10-3	YMM10[pRS413-*ORC2*]	This study
YMM10-4	YMM10[pRS413-*orc2-All-D*]	This study
YMM10-5	YMM10[pRS413-*orc2-All-A*]	This study
YMM10-6	YMM10[pRS413-*orc2–2d*]	This study
YMM10-7	YMM10[pRS413-*orc2-12d*]	This study
YMM10-8	YMM10[pRS413-*orc2-123d*]	This study
YMM10-9	YMM10[pRS413-*orc2-4d*]	This study
YMM10-10	YMM10[pRS413-*orc2-5d*]	This study
YMM10-11	YMM10[pRS413-*orc2-6d*]	This study
YMM10-12	YMM10[pRS413-*orc2-56d*]	This study
YMM10-13	YMM10[pRS413-*orc2-456d*]	This study
YMM10-14	YMM10[pRS413-*orc2-12346d*]	This study
YMM10-15	YMM10[pRS413-*orc2-5a*]	This study
YMM18	DK186 *orc6Δ::TRP1*[pRS416-*ORC6*]	This study
YMM18-2	YMM18[pRS413]	This study
YMM18-3	YMM18[pRS413-*ORC6*]	This study
YMM18-4	YMM18[pRS413-*orc6-All-D*]	This study
YMM18-5	YMM18[pRS413-*orc6-All-A*]	This study
YMM69	YMM10 [pRS425-*GAL1-ORC2-3HA*]	This study
YMM71-1	YMM10 [pRS425-*GAL1-orc2-5d-3HA*]	This study
YMM71-2	YMM10 [pRS425-*GAL1-orc2-5a-3HA*]	This study
YMM76	YMM77 *his3*::pRS403-*orc2-5d-3HA*	This study
YMM77	DK186 *orc2Δ::TRP1 leu2*::pRS405-*GAL1-orc2-1-3FLAG*	This study
YMM84	YMM77 *his3*::pRS403-*ORC2-3HA*	This study
YMM87	W303-1A [pRS425-*GAL1-ORC2-3HA*]	This study
YMM88	W303-1A *cdc28-4* [pRS425-*GAL1-ORC2-3HA*]	This study

immunosorbent assay using the peptide and the peptide lacking the phosphorus at the serine residue (data not shown).

ORCs were co-expressed in *Sf9* cells infected with recombinant baculoviruses and purified as described (29). Baculovirus containing the phospho-mimetic *orc2* gene was constructed using a BD BaculoGold™ transfection kit (BD Biosciences) according to the manufacturer's instructions.

Phosphorylation of ORC—Purification of yeast recombinant CDK (rGST-Cdc28-Clb5) was performed as described (21). The plasmid, pGEX6P-1/*CDC28-CAK1-CKS1-CLB5* was gift from Dr. Araki (National Institute of Genetics). To obtain an active recombinant GST-Cdc28/Clb5 complex (rGST-Cdc28-Clb5), the cell extracts prepared from *Escherichia coli* Rosseta 2(DE)pLysS cells (Novagen) harboring the plasmid was applied to the glutathione-Sepharose column, and rGST-Cdc28-Clb5 was eluted with the buffer containing reduced glutathione.

For phosphorylation of ORC, ORC (30 pmol) and recombinant CDK (13.5 pmol) were incubated at 25 °C for 24 h in the buffer (600 μl) containing 50 mM Hepes-KOH, pH 7.5, 10 mM $MgCl_2$, 1 mM ATP. To remove ATP from ORC samples, ORC was precipitated with SP-Sepharose (GE Healthcare) and eluted with the buffer containing 50 mM Hepes-KOH, pH 7.5, 500 mM KCl, 5 mM $Mg(OAc)_2$, 1 mM EDTA, 1 mM EGTA, 0.02% v/v Nonidet P-40, and 10% v/v glycerol.

UV-cross-linking Assay—UV-cross-linking experiments were done as described previously (28, 29). ORC (3 pmol) was incubated with 4 μM 8-N_3-[γ-^{32}P]ATP in the presence or absence of *ARS1* DNA fragments at 4 °C for 5 min. Samples were placed on Parafilm and subjected to UV irradiation at 4 °C for 2 min. The photolabeling reaction was terminated by the addition of stop solution (70 μl) containing 0.1 M dithiothreitol and 20 mM EDTA. Samples were precipitated by 20% trichloroacetic acid, washed with acetone, and separated by electrophoresis on a polyacrylamide gel (10%) containing SDS. Gels were stained with silver to identify each ORC subunit, and radiolabeled subunits were detected by autoradiography.

Filter Binding Assay—ORC was incubated with [α-^{32}P]ATP or radiolabeled DNA fragments (200 fmol) at 30 °C for 5 min in 40 μl of buffer T (25 mM Tris-HCl, pH 7.6, 5 mM $MgCl_2$, 70 mM KCl, 5 mM dithiothreitol, and 5% (v/v) glycerol). In some of the ATP binding experiments, ORC was further incubated with DNA fragments at 30 °C for 5 min in the same buffer. Samples were passed through nitrocellulose membranes (Millipore HA, 0.45 μm) and washed with 5 ml of ice-cold buffer T twice. The radioactivity remaining on the filter was monitored with a liquid scintillation counter.

ATPase Assay—The ATPase activity of ORC was measured as described previously (28) with some modifications. ORC (0.3 pmol) was incubated with DNA fragments (6 pmol) in 10 μl of ATPase buffer (50 mM Hepes-KOH pH7.6, 150 mM KCl, 5 mM $Mg(OAc)_2$, 1 mM EDTA, 1 mM EGTA, 0.02% v/v Nonidet P-40, and 10 μM radiolabeled ATP) for 60 min at room temperature. The reaction was stopped by the addition of 2% w/v SDS (5 μl), and adenine nucleotides were separated on polyethyleneimine cellulose F TLC plates (Merck).

Chromatin Binding Assay—Yeast spheroplasts were lysed with Triton X-100, and the samples were processed into soluble (supernatant) and chromatin (insoluble precipitate) fractions by centrifugation as previously described (41, 42). Equivalent amounts (total protein) of chromatin fractions were subjected to electrophoresis on a polyacrylamide gel (10%) containing SDS, transferred to polyvinylidene difluoride membranes, and probed with antibodies.

FACS Analysis—The samples were prepared as previously described (33) with some modifications. The cells were pelleted by centrifugation and fixed in 70% ethanol for 1 h. The cells

were pelleted by centrifugation, washed with 50 mM sodium citrate once, pelleted again by centrifugation, incubated with 50 mM sodium citrate containing 0.25 mg/ml RNase A for 1 h at 50 °C, and then treated with 1 mg/ml proteinase K for 1 h at 50 °C. DNA was stained with 50 μg/ml propidium iodide at 4 °C for 1 h, and 20,000 cells from each sample were scanned with a FACSCalibur (BD Biosciences).

Gel Electrophoretic Mobility Shift Assay—A gel electrophoretic mobility shift assay was performed as described (32, 43) with some modifications. ORCs were incubated with adenine nucleotides for 5 min at 30 °C and with radiolabeled wild-type *ARS1* or mutant *ars1/A⁻B1⁻* DNA fragments (100 fmol) for 5 min at 30 °C in 10 μl of buffer T containing 2 mg/ml of bovine serum albumin and 10 μg/ml poly(dI/dC) (nonspecific competitors). The reaction sample was loaded onto a 3.5% polyacrylamide gel containing 0.5 × TBE (0.045 M Tris borate, pH 8.3, and 1 mM EDTA). The gel was electrophoresed for 1.5 h at a constant 200 V, dried, and autoradiographed.

Chromatin immunoprecipitation (ChIP) Assay—A ChIP assay was done as described previously (44) with some modifications. Cells were cross-linked with 1% formaldehyde for 15 min at 25 °C. After the addition of 125 mM (final concentration) glycine, cells were harvested and lysed with glass beads in the buffer (50 mM Hepes-KOH, pH 7.5, 140 mM NaCl, 1 mM EDTA, 1% Triton X-100 (v/v), 0.1% sodium deoxycholate (w/v), 1 mM phenylmethylsulfonyl fluoride, 2 mM benzamidine, 1 μg/ml leupeptin, and 2 μg/ml pepstatin A). Samples were sonicated 30 times for 10 s (to achieve an average fragment size of 0.5–1 kilobases). Immunoprecipitation was performed with magnetic beads which were coated with protein G (Dynal) and antibody against HA or Mcm2p. Precipitates were washed, processed for DNA purification, and subjected to PCR. The PCR cycles included an initial denaturation step of 0.5 min at 95 °C, which was followed by 35 cycles of a denaturation step for 0.5 min at 95 °C, an annealing step for 0.5 min at 50 °C, a polymerization step for 1 min at 72 °C, and a final extension for 4 min at 72 °C. The PCR products were separated on a 3% agarose gel and visualized under UV after ethidium bromide staining.

RESULTS

Site-directed Mutational Analysis of Orc2p and Orc6p Phosphorylation—It was reported that Orc2p and Orc6p have six (Ser-16, Ser-24, Thr-70, Thr-174, Ser-188, and Ser-206) and four (Ser-106, Ser-116, Ser-123, and Thr-146) consensus CDK phosphorylation sites ((S/T)P*X*(K/R)), respectively (Fig. 1*A*). Expression of mutant forms of Orc2p and Orc6p in which these amino acid residues were substituted with Ala caused re-initiation of DNA replication in G_2 phase when a degradation-resistant mutant of Cdc6p and a Mcm7p with an exogenous nuclear localization signal were expressed simultaneously (18, 19). We constructed a phospho-mimetic mutant of Orc2p, Orc2-All-Dp, in which all of the consensus CDK phosphorylation sites were mutated to Asp. Orc6-All-Dp was constructed in a similar way. We also constructed Orc2-All-Ap and Orc6-All-Ap in which the consensus CDK phosphorylation sites were mutated to Ala. Each mutant gene was inserted into a plasmid, and the plasmid was transformed into strain YMM10 (or YMM18) which contains a chromosomal *ORC2* or *ORC6* deletion and an alternative wild-type gene on a plasmid with the *URA3* selectable maker. When the transformants were grown on agar plates containing 5-FOA, the *URA3* plasmid was selected against and lost, causing cells to rely solely on the mutant *orc2* or *orc6* gene (plasmid-shuffling analysis). YMM10 (or YMM18) cells containing plasmid carrying the wild-type genes could grow, and those containing vector only could not grow on the 5-FOA-containing plates (Fig. 1*B*), showing that the plasmid-shuffling system works well. As shown in Fig. 1*B*, YMM10 cells expressing Orc2-All-Dp could grow on agar plates without 5-FOA but not on those with 5-FOA. On the

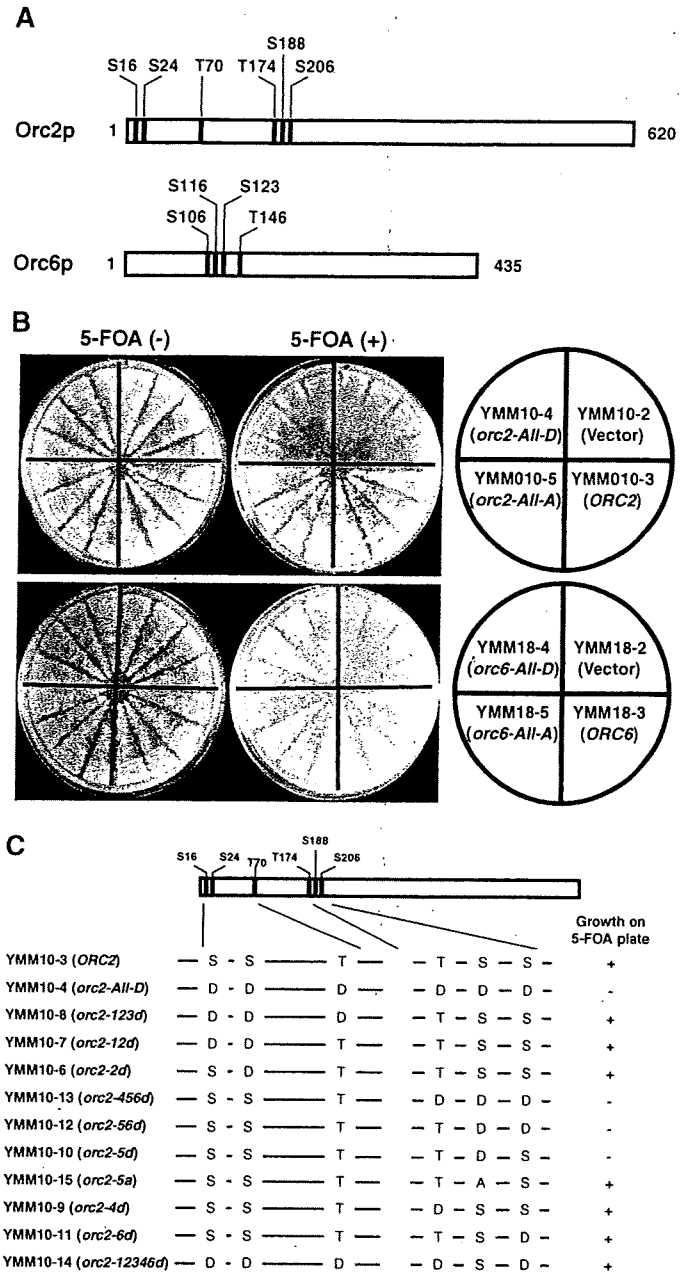

FIGURE 1. **Plasmid shuffling assay for phospho-mimetic *orc2* and *orc6* mutants.** *A*, the positions of consensus CDK phosphorylation sites ((S/T)P*X*(K/R)) in Orc2p and Orc6p are shown. *B*, strains were spread onto synthetic complete agar plates in the arrangement depicted in the *right panel* with or without 5-FOA and incubated at 30 °C for 3 days. *C*, the mutations in the CDK sites of the various Orc2p mutants are indicated, and the results of a plasmid shuffling assay for each Orc2p mutant are shown (C).

42

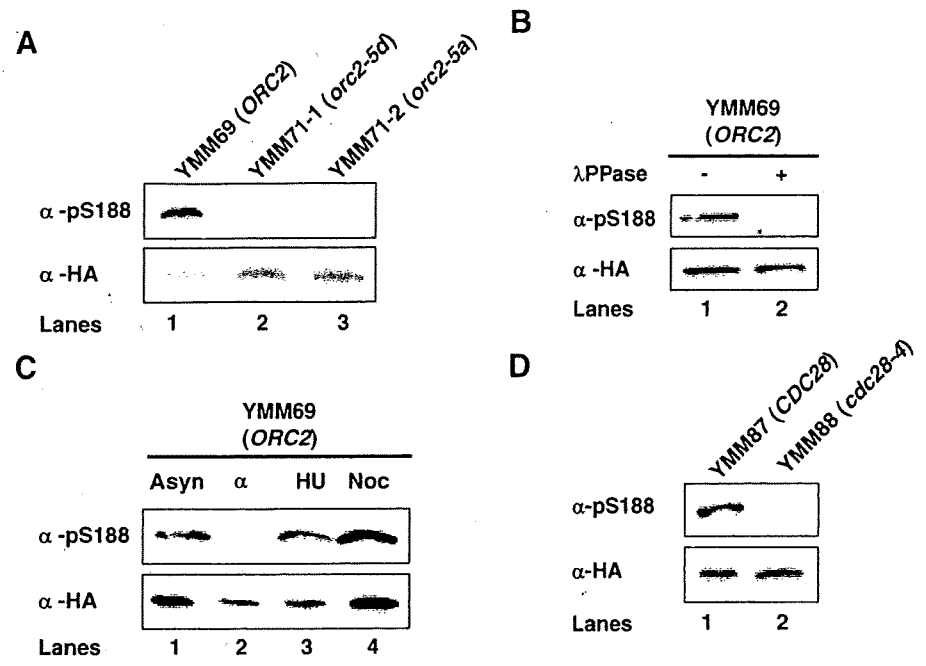

FIGURE 2. **Cell cycle-regulated and CDK-dependent phosphorylation of Ser-188 of Orc2p.** *A*, chromatin fractions were prepared from asynchronously growing YMM69 (*GAL1-ORC2*-3HA), YMM71-1 (*GAL1-orc2-5d*-3HA) and YMM71-2 (*GAL1-orc2-5a*-3HA) cells in YP medium containing galactose. *B*, chromatin fractions prepared from asynchronously growing YMM69 cells in YP medium containing galactose were treated with or without λ-protein phosphatase (*λPPase*) at 30 °C for 1 h. *C*, chromatin fractions were prepared from asynchronously growing and α-factor (*α*)- (or hydroxyurea (*HU*) or nocodazole (*Noc*))-blocked YMM69 cells in YP medium containing galactose. *D*, YMM87 (*CDC28 GAL1-ORC2*-3HA) or YMM88 (*GAL1-cdc28–4 ORC2*-3HA) cells were arrested at G_1 phase by incubation with α-factor in YP medium containing galactose at 23 °C for 4 h, the cells were then released into the same medium containing nocodazole at 37 °C for 2 h, and chromatin fractions were prepared. *A–D*, samples were analyzed by immunoblotting with antibody against Ser-188-phosphorylated Orc2p (α-Ser(P)-188 (*pS188*)).

other hand, YMM18 expressing Orc6-All-Dp could grow even on agar plates containing 5-FOA (Fig. 1*B*). Plasmid shuffling analysis also showed that both of the Ala substitution mutants can support cell growth (Fig. 1*B*), as described previously (18). Based on results in Fig. 1, we consider that dephosphorylation of Orc2p but not of Orc6p is required for cell growth and cell cycle progression.

To identify the amino acid residue responsible for the phenotype exhibited by cells expressing Orc2-All-Dp, we constructed a series of mutant Orc2p, as shown in Fig. 1*C*, and analyzed the function of each mutant protein by plasmid shuffling analysis. Results show that the S188D Orc2p mutant (Orc2-5Dp) but not the variants of Orc2p with mutations in the other consensus CDK phosphorylation sites is unable to support cell growth (Fig. 1*C*). Furthermore, a mutant Orc2p in which all of the consensus CDK phosphorylation sites except the Ser-188 are replaced with Asp (Orc2-12346Dp) could support cell growth (Fig. 1*C*). Thus, we concluded that Ser-188 is an important target of CDK for controlling cell cycle progression, and phosphorylation of this amino acid residue may block cell cycle progression.

To detect phosphorylation of Ser-188 of Orc2p *in vivo*, we prepared polyclonal antibody that recognizes Ser-188-phosphorylated Orc2p (α-Ser(P)-188). As shown in Fig. 2*A*, α-Ser(P)-188 detected a band with the same migration as that detected by antibody against HA in cells expressing wild-type HA-tagged Orc2p but not in cells expressing HA-tagged Ser-188 Orc2p mutant (Orc2-5Dp or Orc2-5Ap). The band was not detected in the wild-type Orc2p-containing sample that had been treated with λ-protein phosphatase (Fig. 2*B*). Based on these results, we conclude that α-Ser(P)-188 can specifically recognize Ser-188-phosphorylated Orc2p. As shown in Fig. 2*C*, Ser-188-phosphorylated Orc2p was detected in asynchronously growing cells, hydroxyurea-blocked cells and nocodazole-blocked cells but not in α mating factor (α-factor)-blocked cells, suggesting that Ser-188 of Orc2p is phosphorylated at the G_1-S boundary and dephosphorylated in late M or G_1 phase. This pattern correlates well with that of cell cycle-regulated phosphorylation of Orc2p, as judged by an upward band shift (18). We also found that Ser-188-phosphorylated Orc2p was not detected in a temperature-sensitive *cdc28* mutant at a non-permissive temperature (Fig. 2*D*), suggesting that the phosphorylation of Ser-188 of Orc2p is catalyzed by CDK.

Function of Orc2-5Dp in Cells—To understand the role of phosphorylation of Orc2p at Ser-188 and the function of Orc2-5Dp in cells, we constructed a YMM76 strain in which the wild-type *ORC2* is deleted, FLAG-tagged Orc2-1p is expressed under control of the *GAL1* promoter and Orc2-5Dp is constitutively expressed. Because Orc2-1p is rapidly degraded at high temperatures (45), YMM76 cells cultured in galactose-free medium at 37 °C rely on Orc2-5Dp. YMM84 cells express wild-type Orc2p instead of Orc2-5Dp, and YMM77 strain was used as the control.

We characterized these strains by a chromatin binding assay. As shown in Fig. 3*A*, incubation of the strains (YMM84 (*ORC2*), YMM76 (*orc2-5d*), and YMM77 (*orc2Δ*)) at 37 °C in glucose-containing medium caused the rapid disappearance of FLAG-tagged Orc2-1p. Expression of HA-tagged wild-type Orc2p or Orc2-5Dp was induced under these conditions, suggesting that yeast cells have an as yet an unknown mechanism for keeping the amount of Orc2p at a constant level. A similar mechanism seems to exist in human cells based on a recent report (46). Results similar to those in Fig. 3*A* were observed when total cell lysates were used instead of chromatin fractions (data not shown). The results in Fig. 3*A* also show that Orc2-5Dp (maybe as a complex with other subunits of ORC) can bind to chromatin as efficiently as wild-type Orc2p. Along with the degradation of FLAG-tagged Orc2-1p, Orc3p was degraded in YMM77 but not as distinctly in YMM76 cells (Fig. 3*A*), supporting the idea that Orc2-5Dp can form a complex with other ORC subunits because the ORC becomes unstable when one of its subunits is missing (47).

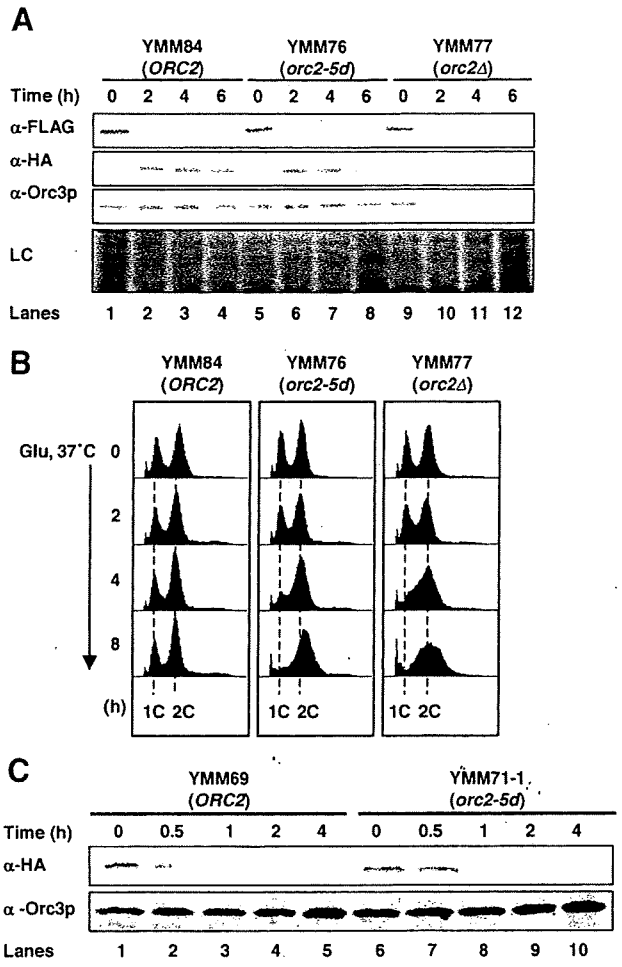

FIGURE 3. **FACS analysis of *orc2-5d* strain.** *A* and *B*, YMM84 (*GAL1-orc2-1-FLAG, ORC2–3HA*), YMM76 (*GAL-orc2-1-FLAG, orc2-5d-3HA*), and YMM77 (*GAL-2-1-FLAG*) grown in YP medium containing galactose were further incubated at 37 °C in YP medium containing glucose (*Glu*) for the indicated periods. FLAG-tagged Orc2-1p, HA-tagged Orc2p (or Orc2-5Dp), and Orc3p in chromatin fractions were detected by immunoblotting with antibody against FLAG, HA, or Orc3p. *A*, for loading control, the gel was stained with silver. *B*, cell cycle progression was examined by FACS analysis. *C*, YMM69 (*GAL1-ORC2*-3HA) and YMM71-1 (*GAL1-orc2-5d*-3HA) cells grown in YP medium containing galactose were further incubated at 37 °C in YP medium containing glucose for the indicated periods. Whole cell extracts were prepared and analyzed by immunoblotting with antibody against HA and Orc3p.

FACS analysis showed that incubation of YMM76 cells in glucose-containing medium at 37 °C causes accumulation of cells with 2C DNA content (Fig. 3*B*), suggesting that most of these cells were blocked at G_2/M phase. Similar accumulation was observed in YMM77 cells, as described previously (45). Furthermore, we examined the stability of Orc2-5Dp in cells. As shown in Fig. 3*C*, after the expression of Orc2-5Dp or wild-type Orc2p was shut off, the time-course profile of degradation of Orc2-5Dp was indistinguishable from that of wild-type Orc2p, suggesting that Orc2-5Dp is as stable as wild-type Orc2p.

We performed block and release experiments to examine the cell cycle progression in detail. Asynchronously cultured cells were synchronized at G_1 or G_2/M phase by incubation with α-factor (Fig. 4, *D* and *E*) or nocodazole (Fig. 4, *B* and *C*), respectively, expression of Orc2-1p was suppressed by incubating cells in galactose-free medium, and then the cells were released into fresh medium (Fig. 4*A*). As shown in Fig. 4*B*, G_2/M-G_1 progression was indistinguishable between the YMM76 and YMM84 strains. However, the following G_1-S transition and S phase progression was a little slower in the YMM76 than in the YMM84 strain (see the FACS data for 50 or 60 min after the release; Fig. 4*B*). The delay was more apparent in the *orc2Δ* strain (Fig. 4*B*). A chromatin binding assay confirmed that Orc2-1p disappeared before the release, and approximately equal amounts of wild-type Orc2p and Orc2-5Dp were loaded on the chromatin (Fig. 4*C*). Results similar to those in Fig. 4*C* were observed when total cell lysates were used instead of chromatin fractions (data not shown). On the other hand, data from α-factor block experiments showed that the G_1-S transition and S phase progression was not so different between these two strains (YMM76 and YMM84) (Fig. 4*D*), suggesting that Orc2-5Dp can support the initiation of DNA replication after the point of the cell cycle which is blocked by α-factor; thus, after pre-RC formation. Thus, expression of Orc2-5Dp in late M or early G_1 phase seems to suppress G_1-S transition and S phase progression, maybe through inhibiting pre-RC formation.

It is well known that various checkpoint responses exist to achieve proper cell cycle progression. For example, DNA replication stress, DNA damage, or defects in spindle attachment to centromeres induce the checkpoint response to arrest cell cycle progression at G_2/M phase through phosphorylation of Rad53p (48). A number of previous reports show that dysfunction of ORC induces phosphorylation of Rad53p and some cell cycle checkpoint responses (45, 49–52). Thus, the results shown in Fig. 3*B* suggest that some cell cycle checkpoint responses are induced by the experimental conditions. To test this possibility, we monitored the level of phosphorylation of Rad53p by immunoblotting. As shown in Fig. 4*F*, induction of phosphorylation of Rad53p was observed in the YMM76 strain after release, suggesting that some Rad53p-mediated checkpoint responses are induced and that this induction is involved in conferring the phenotype of accumulation of cells with 2C content in this strain. A high level of Rad53p phosphorylation was observed in cells lacking Orc2p or hydroxyurea-treated cells (Fig. 4*F*), as described previously (45).

To examine the activity of Orc2-5Dp in origin binding and pre-RC formation, we performed the experiments shown in Fig. 5*A*; asynchronously cultured cells (YMM84, YMM76, and YMM77) were synchronized at G_2/M phase, expression of Orc2-1p was suppressed, and cells were released into fresh medium with α-factor to re-synchronize at G_1 phase. FACS analysis showed that these synchronizations were well controlled (Fig. 5*B*). Under the same conditions we performed a ChIP assay; HA-tagged Orc2p or Orc2-5Dp was precipitated, and co-precipitated DNA species were monitored by PCR. As shown in Fig. 5*C*, both *ARS1* (origin) and *LEU2* (control) DNA fragments were approximately equally amplified when total DNA prepared from these strains was used as a template, but relative higher amplification of *ARS1* DNA fragments was observed when DNA immunoprecipitated with an antibody against HA was used as a template, showing that a ChIP assay system had been established. Not only *LEU2* but also *ARS1* DNA fragments were amplified approximately equally between the YMM84 and YMM76 strains (Fig. 5*C*). On the other hand,

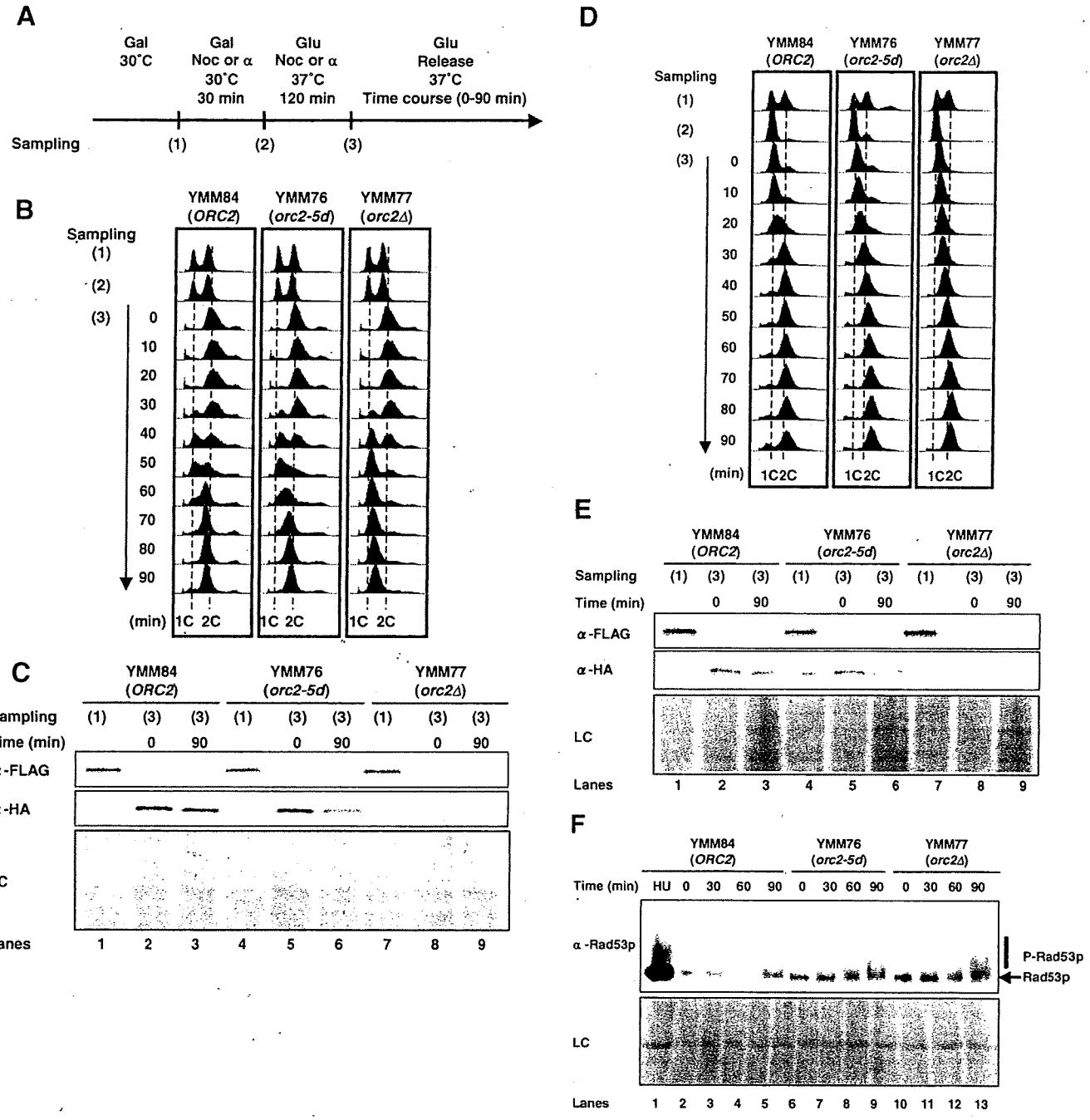

FIGURE 4. **Cell cycle progression in *orc2-5d* strain.** *A*, experimental outline and timing of sampling. YMM84 (*GAL1–2-1-FLAG, ORC2-3HA*), YMM76 (*GAL-orc2-1-FLAG, orc2-5d-3HA*), and YMM77 (*GAL-orc2-1-FLAG*) cells were incubated in YP medium containing galactose (*Gal*) and nocodazole (*Noc*) (*B* and *C*) or α-factor (α) (*D–F*) at 30 °C for 30 min and then incubated in YP medium containing glucose (*Glu*) and the same concentration of each blocker at 37 °C for 120 min. Cells were released into YP medium containing glucose and incubated at 37 °C for the indicated periods. Samples were analyzed by FACS (*B* and *D*). FLAG-tagged Orc2-1p and HA-tagged Orc2p (or Orc2-5Dp) in the chromatin fractions were detected as described in the legend of Fig. 3 (*C* and *E*). Whole cell extracts were analyzed by immunoblotting with antibody against Rad53p. *F*, the *arrow* and *vertical line* indicate unphosphorylated and phosphorylated, respectively, Rad53p.

less efficient amplification of *ARS1* DNA fragments was observed in the YMM77 strain (Fig. 5*C*). These results suggest that ORC containing Orc2-5Dp can specifically bind to origin DNA in a similar way to wild-type ORC.

We performed a chromatin binding assay to monitor pre-RC formation; the amounts of ORC and MCM in the chromatin fractions were monitored by immunoblotting. As shown in Fig. 5*D*, the amount of Orc2-5Dp in chromatin fractions was much the same as that of wild-type Orc2p, confirming that ORC containing Orc2-5Dp can bind to origin DNA in an equivalent way to wild-type ORC. On the other hand, the amount of Mcm2p in the chromatin fractions of YMM76 was less than that in YMM84 at G_1 phase, suggesting that MCM loading on chromatin and pre-RC formation is inhibited in YMM76. Unfortunately, because ChIP assay for any subunits of MCM did not work in our strains, we could not confirm the results of chromatin binding assay by ChIP assay. These results suggest that ORC containing Orc2-5Dp is inefficient for pre-RC formation,

45

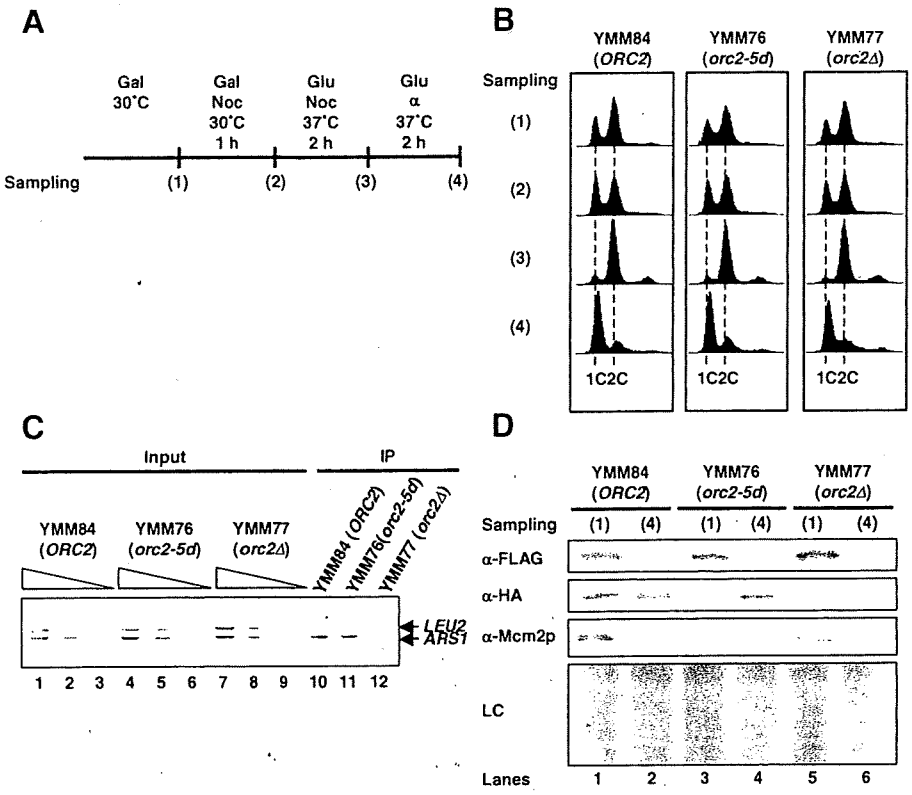

FIGURE 5. **Pre-RC formation in the *orc2-5d* strain.** *A*, experimental outline and timing of sampling. YMM84 (*GAL1-orc2-1-FLAG, ORC2–3HA*), YMM76 (*GAL-orc2-1-FLAG, orc2-5d-3HA*), and YMM77 (*GAL-orc2-1-FLAG*) cells were incubated in YP medium containing galactose (*Gal*) and nocodazole (*Noc*) at 30 °C for 1 h and then incubated in YP medium containing glucose (*Glu*) and the same concentration of nocodazole at 37 °C for 2 h. *B–D*, cells were released into YP medium containing glucose and α-factor (α) and incubated at 37 °C for 2 h. *B*, samples were analyzed by FACS. DNA fractions (at the timing of *4*) were prepared from the immunoprecipitated samples with antibody against HA and whole cell extracts (*Input*) and subjected to PCR with specific primer sets for *LEU2* and *ARS1*. *C*, titration of the input DNA is shown by the *triangle symbols*. The PCR products were separated on a 3% agarose gel and visualized under UV. *D*, FLAG-tagged Orc2-1p, HA-tagged Orc2p (or Orc2-5Dp), and Mcm2p in chromatin fractions were detected as described in the legend of Fig. 3.

and we consider that dephosphorylation of Ser-188 of Orc2p at late M or G_1 phase is important for pre-RC formation.

Biochemical Characterization of ORC2-5D—We named the ORC containing Orc2-5Dp, ORC2-5D, and purified both ORC2-5D and wild-type ORC from insect cells overexpressing each type of ORC. As shown in Fig. 6*A*, both types of ORC were prepared to similar purity, and no apparent degradation of subunits was observed.

The DNA binding properties of wild-type ORC and ORC2-5D were studied using a filter binding assay with radiolabeled origin DNA (*ARS1*). *ARS1* contains four elements important for its origin function (A, B1, B2, and B3) (53), of which A and B1 are ORC binding sites (5, 54). We examined the extent of binding of each ORC to radiolabeled wild-type *ARS1* or mutant *ars1/A⁻B1⁻* DNA fragments in the presence of various concentrations of a nonspecific competitor DNA, poly(dI/dC) (Fig. 6*B*). Both the wild-type ORC and ORC2-5D bound to wild-type *ARS1* more efficiently than to mutant *ars1/A⁻B1* DNA fragments, suggesting that ORC2-5D can specifically bind to origin DNA. These results are consistent with *in vivo* data showing that ORC binding to origin DNA is indistinguishable between YMM76 and YMM84 strains (Fig. 5).

We also compared the DNA binding activities of ORC2-5D, wild-type ORC, ORC-1A (an ORC that contains the mutant Orc1p with a defective Walker A motif), and ORC-5A (an ORC that contains the mutant Orc5p with a defective Walker A motif) by a gel electrophoretic mobility shift assay. As shown in Fig. 6*C*, in the presence of ATP, wild-type ORC and ORC-5A but not ORC-1A bound to wild-type *ARS1* but not to mutant *ars1/A⁻B1* DNA fragments. All of these ORCs did not bind to any DNA fragments in the presence of ADP, as described previously (32). The DNA binding properties of ORC2-5D were indistinguishable from that of wild-type ORC even in the gel electrophoretic mobility shift assay (Fig. 6*C*), confirming that ORC2-5D can specifically bind to origin DNA.

The ATP binding properties of the wild-type ORC and ORC2-5D were also compared using a filter binding assay. Both types of ORC showed high affinity for ATP, but the number of ATP molecules bound to each ORC2-5D was less than to wild-type ORC in the presence of high concentrations of ATP (Fig. 7*A*). Scatchard plot analysis showed that the K_d values of wild-type ORC and ORC2-5D for ATP were 17 and 16 nM, respectively, and that the ATP binding sites per wild-type ORC and ORC2-5D were 0.35 and 0.18, respectively. These results suggest that ATP binding to either Orc1p or Orc5p is inhibited in ORC2-5D, and we speculated that ATP binding to Orc5p is inhibited in ORC2-5D, because ORC2-5D can specifically bind to origin DNA (Fig. 6), which is independent of Orc5p ATP binding.

To test this idea, we performed UV-cross-linking analysis using radiolabeled 8-N_3-ATP. As shown in Fig. 7*B*, the results for the wild-type ORC were similar to those reported previously (28); Orc1p, Orc4p, and Orc5p were labeled in the presence of origin DNA fragments, and the labeling of Orc1p and Orc4p was less in the absence of origin DNA fragments. For ORC2-5D, Orc1p and Orc4p but not Orc5p were labeled in the presence of origin DNA fragments, supporting the idea that ATP binding to Orc5p is inhibited in ORC2-5D.

It has been reported that origin DNA fragments stimulate ATP binding to Orc1p (28, 29). We, therefore, examined the effect of *ARS1* and mutant *ars1/A⁻B1⁻* DNA fragments on ATP binding to wild-type ORC and ORC2-5D. As shown in Fig. 7*C*, *ARS1* DNA fragments increased the amount of ATP bound to wild-type ORC, and mutant *ars1/A⁻B1⁻* DNA fragments produced a smaller increase, as reported previ-

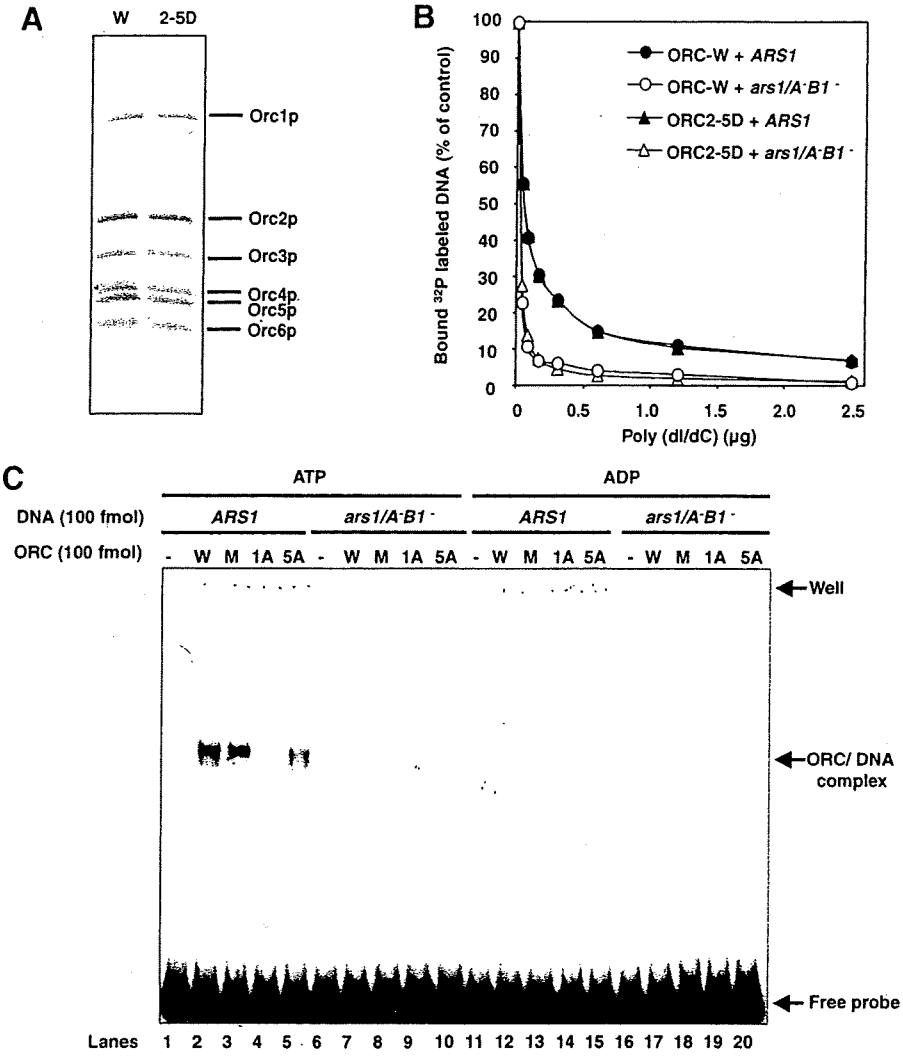

FIGURE 6. **DNA binding activity of ORC2-5D.** *A*, 1 pmol of wild-type ORC (*W*) and ORC2-5D (*2–5D*) were electrophoresed on a 7.5% SDS-polyacrylamide gel and stained with silver. *B*, wild-type ORC and ORC2-5D (0.2 pmol) were incubated with 200 fmol of radiolabeled *ARS1* or *ars1/A⁻B1⁻* DNA at 30 °C for 5 min in the presence of the indicated amounts of competitor DNA, poly (dI/dC). the amounts of DNA bound to each ORC were determined by filter binding assay. The amounts of DNA bound in the absence of poly(dI/dC) were 128 fmol (*closed circles*), 53 fmol (*open circles*), 100 fmol (*closed triangles*) and 45 fmol (*open triangles*). *C*, wild-type ORC (*W*), ORC2-5D (*M*), ORC-1A (*1A*), and ORC-5A (*5A*) were incubated with radiolabeled *ARS1* or *ars1/A⁻B1⁻* DNA fragments in the presence of 0.3 μg poly (dI/dC). Samples were electrophoresed on a 3.5% polyacrylamide gel and autoradiographed.

ously (28, 29). Both types of DNA fragments affected ATP binding to ORC2-5D in a similar way (Fig. 7*C*), suggesting that the *orc2-5d* mutation affects neither ATP binding to Orc1p nor DNA binding to the ORC.

We measured the ATPase activity. As shown in Fig. 7*D*, ORC2-5D showed a similar level of ATPase activity as wild-type ORC, and ORC-1A showed no ATPase activity, as reported previously (28). It has been reported that double-stranded *ARS1* DNA fragments inhibit the ATPase activity of ORC (28). Here we examined the effect of double-stranded *ARS1* DNA fragments on the ATPase activity of ORC2-5D. *ARS1* DNA fragments inhibited the ATPase activity of wild-type ORC and ORC2-5D in a similar way (Fig. 7*D*). The results suggest that the *orc2-5d* mutation affects neither the ATPase activity of ORC nor origin DNA binding to ORC. All of the data from the *in vitro* experiments show that although ORC2-5D has normal origin DNA binding, ATP binding to Orc1p, and ATPase activities, it is inert for ATP binding to Orc5p.

We also examined the effect of Ser-188 phosphorylation of Orc2p on biochemical characters ORC. For phosphorylation of ORC, wild-type ORC was treated with yeast recombinant CDK (rGST-Cdc28-Clb5). This treatment increased the band intensity of Orc2p in immunoblotting analysis with α-Ser(P)-188 (Fig. 8*B*) without apparent degradation of each subunit of ORC (Fig. 8*A*). A filter binding assay revealed that phosphorylation of wild-type ORC decreased the amount of bound ATP (Fig. 8*C*). UV-cross-linking analysis revealed that phosphorylation of wild-type ORC inhibited the labeling of Orc5p in both the presence and absence of origin DNA fragments (Fig. 8*D*). On the other hand, phosphorylation of wild-type ORC did not affect its binding to wild-type *ARS1* DNA fragments (Fig. 8*E*). Results in Fig. 8 suggest phosphorylated wild-type ORC is less active for ATP binding to Orc5p than unphosphorylated wild-type ORC. Combining data in Figs. 6–8, it is suggested that Ser-188 phosphorylation of Orc2p of wild-type ORC inhibits ATP binding to Orc5p.

The result in Fig. 2*A* suggests that ORC2-5D cannot be detected in immunoblotting analysis with α-Ser(P)-188. As shown in supplemental Fig. S1*A*, ORC2-5D (3 pmol) was not detected in immunoblotting analysis with α-Ser(P)-188 under the conditions in which wild-type ORC (0.3 pmol) was detected, supporting the idea mentioned above. On the other hand, treatment of wild-type ORC with λ-protein phosphatase decreased the band intensity in this analysis (data not shown), suggesting that wild-type ORC purified from *Sf9* cells is partially phosphorylated at Ser-188 of Orc2p. Therefore, we compared wild-type ORC treated with λ-protein phosphatase to ORC2-5D in immunoblotting analysis with α-Ser(P)-188. As shown in supplemental Fig. S1B, wild-type ORC treated with λ-protein phosphatase is less reactive than ORC2-5D in this assay. These results suggest that ORC2-5D is more reactive to α-Ser(P)-188 than Ser-188-unphosphorylated wild-type ORC; however, it is less reactive than Ser-188-phosphorylated wild-type ORC, suggesting that α-Ser(P)-188 preferentially recognizes phosphorylated Ser-188, comparing to Asp-188 in Orc2p.

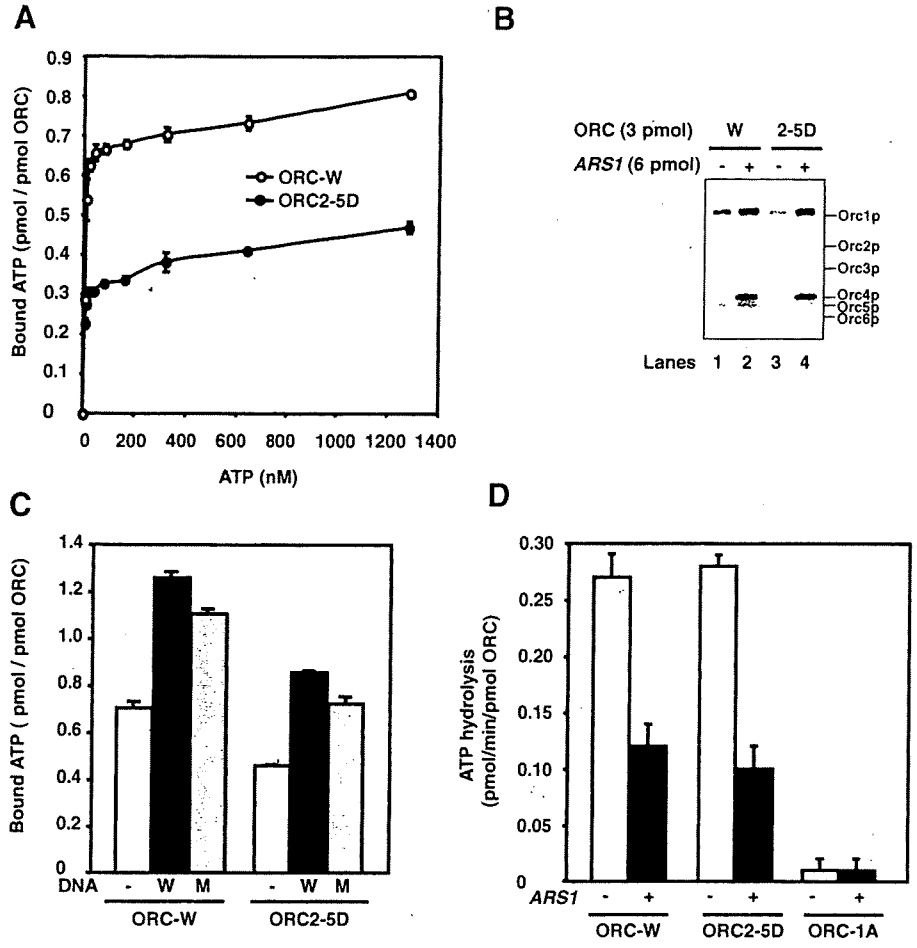

FIGURE 7. **ATP binding activity of ORC2-5D.** *A*, wild-type ORC (*ORC-W*) and ORC2-5D were incubated with radiolabeled ATP as indicated, and the amount of ATP attached to the ORC was determined by the filter binding assay. Values are the mean ± S.D. (n = 3). *B*, wild-type ORC (*W*) and ORC2-5D (*2–5D*) (3 pmol) were incubated with 4 μM 8-N_3-[γ-^{32}P]ATP in the presence or absence of 6 pmol of *ARS1* DNA fragments at 4 °C for 10 min. After UV-cross-linking, samples were separated by SDS-polyacrylamide gel (10%) electrophoresis and followed by autoradiography to identify labeled subunits. *C*, wild-type ORC (*ORC-W*) and ORC2-5D (0.5 pmol) were incubated with 0.5 μM radiolabeled ATP in the presence or absence of 0.5 pmol of *ARS1* (*W*) or *ars1/A*$^-$*B1*$^-$ (*M*) DNA fragments at 30 °C for 5 min, and the amount of ATP attached to the ORC was determined by the filter binding assay. Values are the mean ± S.D. (n = 3). *D*, wild-type ORC (*ORC-W*), ORC2-5D, and ORC-1A (0.5 pmol) were incubated with 10 μM radiolabeled ATP in the presence or absence of 6 pmol of *ARS1* DNA fragments. ATPase activity is shown as ATP hydrolyzed/min/pmol of ORC. Values are the mean ± S.D. (n = 3).

DISCUSSION

Using mutant forms of Orc2p and Orc6p in which all the consensus CDK phosphorylated sites are substituted with Ala, which are unable to be phosphorylated, Nguyen *et al.* (18) suggested that phosphorylation of these subunits is important for suppression of re-initiation of chromosomal DNA replication at G_2/M phase. Expression of these Orc2p and Orc6p mutants with the degradation-resistant mutant Cdc6p and the Mcm7p with exogenous nuclear localization signal induces re-initiation of chromosomal DNA replication (18). However, it is unclear which subunit and which amino acid residues are responsible for this regulation. Furthermore, the role of dephosphorylation of ORC in late M or G_1 phase cannot be revealed with this type of mutant proteins. In this study, by using mutant forms of Orc2p and Orc6p in which the CDK phosphorylated sites are substituted with Asp, phospho-mimetic mutants of Orc2p and Orc6p, we have suggested that phosphorylation of Orc2p but not of Orc6p is important for the regulation of cell cycle progression. Furthermore, analysis of phospho-mimetic Orc2p mutants for each of these CDK phosphorylated sites suggested that of these sites, Ser-188 of Orc2p is important. Ser-188 is phosphorylated at the G_1-S boundary and dephosphorylated at the late M or G_1 phase, and expression of the phospho-mimetic Orc2p mutant for this amino acid residue (Orc2-5Dp) delayed cell cycle progression. Furthermore, we found that expression of Orc2-5Dp delayed the G_1-S transition (and S phase progression), suggesting that dephosphorylation of Ser-188 of Orc2p is important for pre-RC formation. These are the first data suggesting that dephosphorylation of ORC is involved in regulation of initiation of DNA replication. It is reasonable to speculate that the phosphorylation of Ser-188 of Orc2p at the G_1-S boundary is involved in suppression of re-initiation of DNA replication at the G_2/M phase.

The YMM76 strain, which expresses Orc2-5Dp instead of wild-type Orc2p, showed a phenotype of accumulation of cells with 2C DNA content, suggesting that cell cycle progression is delayed at the G_2/M phase. We also showed that phosphorylation of Rad53p is stimulated in the YMM76 strain, suggesting that some Rad53p-mediated cell cycle checkpoint responses are induced in this strain. It has been reported that ORC dysfunction causes less efficient formation of pre-RC, which in turn induces DNA damage, replication arrest, and spindle assembly checkpoint responses, resulting in cell cycle arrest at the G_2/M phase (45, 50–52). Thus, it seems that checkpoint responses induced by inefficient formation of the pre-RC due to expression of Orc2-5Dp is responsible for the phenotype of accumulation of cells with 2C DNA content. It is also possible that the phenotype is due to a defect in sister-chromatid cohesion, because a recent report showed that ORC plays an important role in this process (45).

Biochemical analysis of ORC2-5D provided surprising results that ORC2-5D is defective in Orc5p ATP binding, suggesting that the phosphorylation of Ser-188 of Orc2p inhibits ATP binding to Orc5p. Data with Ser-188-phosphorylated wild-type ORC supported this idea. Both ATP binding and phosphorylation of ORC is important for regulating ORC function, and this is the first evidence for a link between them. ORC2-5D binds to origin DNA normally both *in vitro* and *in vivo*, and ORC2-5D retains the high affinity of Orc1p for ATP and ATPase activity.

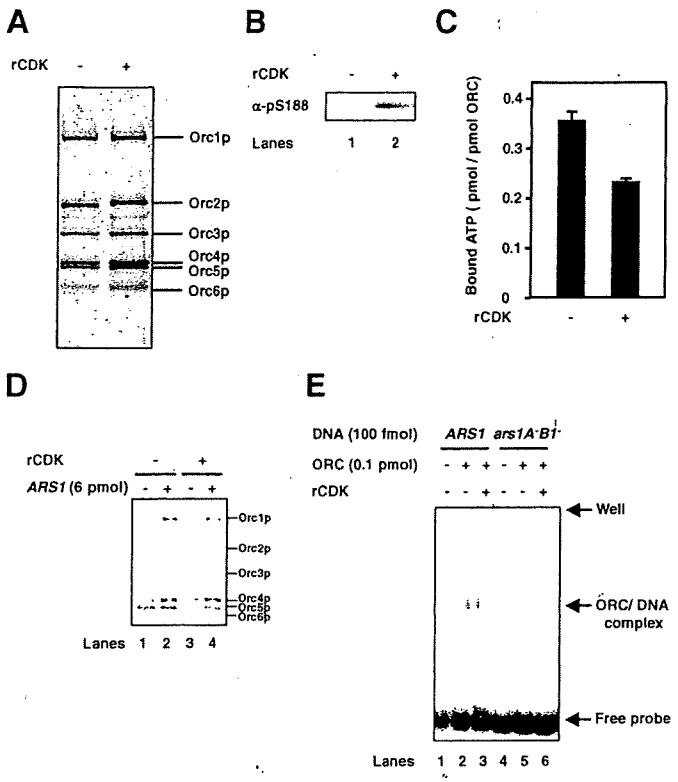

FIGURE 8. **Effect of phosphorylation of ORC on its biochemical characters.** *A–E*, wild-type ORC was incubated with or without recombinant CDK (*rCDK*). One pmol of wild-type ORC was electrophoresed and analyzed with silver stain (*A*) or immunoblotting with α-Ser(P)-188 (*α-pS188*; *B*) as described in the legend of Figs. 6 or 2, respectively. *C*, ATP binding to ORC (1 pmol) and 0.5 μM ATP was examined as described in the legend of Fig. 7. Values are the mean ± S.D. (n = 3). *D*, UV-cross-linking analysis was done for ORC (3 pmol) as described in the legend of Fig. 7. *E*, gel electrophoretic mobility shift assay was done as described in the legend of Fig. 6.

Furthermore, we have previously suggested that Orc2p phosphorylation does not affect its binding to other ORC subunits (36). Thus, the mutation in ORC2-5D does not seem to drastically affect the higher order structure of ORC and non-specifically diminish ORC function. At present, it is not clear how Orc2p phosphorylation affects the binding of ATP to Orc5p. Because our previous yeast two-hybrid analysis showed that Orc2p has a strong interaction with Orc5p (36), it is possible that phosphorylation of Orc2p affects the structure of Orc5p resulting in it losing its affinity for ATP. We recently reported that ORC-5A (ORC containing a mutant Orc5p with a defective Walker A motif) is unstable in cells due to degradation by the ubiquitin-proteasome system (33, 34). However, we have shown here that ORC2-5D is stable in cells. Because Orc5-Ap showed decreased affinity for Orc4p by yeast two-hybrid analysis (36), one possibility is that the mutation in ORC-5A affects its interaction with Orc4p in a manner that is independent of ATP binding to Orc5p, which is responsible for its instability in cells. Supporting this notion, we have previously shown that overexpression of Orc4p suppresses the growth defect phenotype of the *orc5-A* strain (33) but not that of the *orc2-5d* strain (data not shown in this paper). One remaining unsolved question is whether the defect in ATP binding to Orc5p is responsible for the phenotype exhibited by the *orc2-5d* strain, such as a slow G_1-S transition, induction of phosphorylation of Rad53p, and inefficient loading of MCM onto chromatin. It was shown that ORC can directly interact with Cdc6p, Cdt1p, and Mcm2p and that these interactions are important for pre-RC formation (35, 55, 56). Analysis of a suppressor mutant for the *orc2-5d* strain and biochemical analysis of the effects of ATP binding to Orc5p on the interactions between ORC-Cdc6p, ORC-Cdt1p, and ORC-MCM will be important to address this issue. Cell cycle-regulated fluctuation in CDK activity is a key event for regulation of initiation of DNA replication. Activation of CDK at the G_1-S boundary is important for initiation of DNA replication through phosphorylation of Sld2p and Sld3p (20–22). Maintenance of this high level of CDK activity is important for suppression of re-initiation at G_2/M phase through phosphorylation of Orc2p, Cdc6p, and MCM. The results of this study also suggest that dephosphorylation of Orc2p at late M or G_1 phase is important for the formation of pre-RC.

Acknowledgments—We thank Dr. Bruce Stillman (Cold Spring Harbor Laboratory) for providing antibodies, Dr. Stephen P. Bell (Massachusetts of Technology) for providing a recombinant baculovirus, Dr. Hiroyuki Araki (National Institute of Genetics) for providing a plasmid, and Dr. Joachim Li (University of California, San Francisco) for providing strains.

REFERENCES

1. Kelly, T. J., and Brown, G. W. (2000) *Annu. Rev. Biochem.* **69**, 829–880
2. Bell, S. P., and Dutta, A. (2002) *Annu. Rev. Biochem.* **71**, 333–374
3. Dutta, A., and Bell, S. P. (1997) *Annu. Rev. Cell Dev. Biol.* **13**, 293–332
4. Diffley, J. F. (2004) *Curr. Biol.* **14**, 778–786
5. Bell, S. P., and Stillman, B. (1992) *Nature* **357**, 128–134
6. Dahmann, C., Diffley, J. F., and Nasmyth, K. A. (1995) *Curr. Biol.* **5**, 1257–1269
7. Noton, E., and Diffley, J. F. (2000) *Mol. Cell* **5**, 85–95
8. Weinreich, M., Liang, C., Chen, H. H., and Stillman, B. (2001) *Proc. Natl. Acad. Sci. U. S. A.* **98**, 11211–11217
9. Mimura, S., Seki, T., Tanaka, S., and Diffley, J. F. (2004) *Nature* **431**, 1118–1123
10. Wilmes, G. M., Archambault, V., Austin, R. J., Jacobson, M. D., Bell, S. P., and Cross, F. R. (2004) *Genes Dev.* **18**, 981–991
11. Elsasser, S., Chi, Y., Yang, P., and Campbell, J. L. (1999) *Mol. Biol. Cell* **10**, 3263–3277
12. Sanchez, M., Calzada, A., and Bueno, A. (1999) *J. Biol. Chem.* **274**, 9092–9097
13. Drury, L. S., Perkins, G., and Diffley, J. F. (1997) *EMBO J.* **16**, 5966–5976
14. Drury, L. S., Perkins, G., and Diffley, J. F. (2000) *Curr. Biol.* **10**, 231–240
15. Nguyen, V. Q., Co, C., Irie, K., and Li, J. J. (2000) *Curr. Biol.* **10**, 195–205
16. Liku, M. E., Nguyen, V. Q., Rosales, A. W., Irie, K., and Li, J. J. (2005) *Mol. Biol. Cell* **16**, 5026–5039
17. Labib, K., Diffley, J. F., and Kearsey, S. E. (1999) *Nat. Cell Biol.* **1**, 415–422
18. Nguyen, V. Q., Co, C., and Li, J. J. (2001) *Nature* **411**, 1068–1073
19. Archambault, V., Ikui, A. E., Drapkin, B. J., and Cross, F. R. (2005) *Mol. Cell. Biol.* **25**, 6707–6721
20. Tanaka, S., Umemori, T., Hirai, K., Muramatsu, S., Kamimura, Y., and Araki, H. (2007) *Nature* **445**, 328–332
21. Tak, Y. S., Tanaka, Y., Endo, S., Kamimura, Y., and Araki, H. (2006) *EMBO J.* **25**, 1987–1996
22. Masumoto, H., Muramatsu, S., Kamimura, Y., and Araki, H. (2002) *Nature* **415**, 651–655
23. Sekimizu, K., Bramhill, D., and Kornberg, A. (1987) *Cell* **50**, 259–265
24. Mizushima, T., Sasaki, S., Ohishi, H., Kobayashi, M., Katayama, T., Miki, T., Maeda, M., and Sekimizu, K. (1996) *J. Biol. Chem.* **271**, 25178–25183
25. Mizushima, T., Takaki, T., Kubota, T., Tsuchiya, T., Miki, T., Katayama, T., and Sekimizu, K. (1998) *J. Biol. Chem.* **273**, 20847–20851
26. Katayama, T., Kubota, T., Kurokawa, K., Crooke, E., and Sekimizu, K.

(1998) *Cell* **94,** 61–71
27. Mizushima, T., Nishida, S., Kurokawa, K., Katayama, T., Miki, T., and Sekimizu, K. (1997) *EMBO J.* **16,** 3724–3730
28. Klemm, R. D., Austin, R. J., and Bell, S. P. (1997) *Cell* **88,** 493–502
29. Makise, M., Takenaka, H., Kuwae, W., Takahashi, N., Tsuchiya, T., and Mizushima, T. (2003) *J. Biol. Chem.* **278,** 46440–46445
30. Bowers, J. L., Randell, J. C., Chen, S., and Bell, S. P. (2004) *Mol. Cell* **16,** 967–978
31. Randell, J. C., Bowers, J. L., Rodriguez, H. K., and Bell, S. P. (2006) *Mol. Cell* **21,** 29–39
32. Takenaka, H., Makise, M., Kuwae, W., Takahashi, N., Tsuchiya, T., and Mizushima, T. (2004) *J. Mol. Biol.* **340,** 29–37
33. Takahashi, N., Yamaguchi, Y., Yamairi, F., Makise, M., Takenaka, H., Tsuchiya, T., and Mizushima, T. (2004) *J. Biol. Chem.* **279,** 8469–8477
34. Makise, M., Takahashi, N., Matsuda, K., Yamairi, F., Suzuki, K., Tsuchiya, T., and Mizushima, T. (2007) *Biochem. J.* **402,** 397–403
35. Mizushima, T., Takahashi, N., and Stillman, B. (2000) *Genes Dev.* **14,** 1631–1641
36. Matsuda, K., Makise, M., Sueyasu, Y., Takehara, M., Asano, T., and Mizushima, T. (2007) *FEMS Yeast Res.* **7,** 1263–1269
37. Thomas, B. J., and Rothstein, R. (1989) *Cell* **56,** 619–630
38. Liang, C., Weinreich, M., and Stillman, B. (1995) *Cell* **81,** 667–676
39. Sikorski, R. S., and Hieter, P. (1989) *Genetics* **122,** 19–27
40. Kuniyasu, A., Kaneko, K., Kawahara, K., and Nakayama, H. (2003) *FEBS Lett.* **552,** 259–263
41. Liang, C., and Stillman, B. (1997) *Genes Dev.* **11,** 3375–3386
42. Takahashi, N., Tsutsumi, S., Tsuchiya, T., Stillman, B., and Mizushima, T. (2002) *J. Biol. Chem.* **277,** 16033–16040
43. Lee, J. R., Makise, M., Takenaka, H., Takahashi, N., Yamaguchi, Y., Tsuchiya, T., and Mizushima, T. (2002) *Biochem. J.* **362,** 395–399
44. Aparicio, O. M., Weinstein, D. M., and Bell, S. P. (1997) *Cell* **91,** 59–69
45. Shimada, K., and Gasser, S. M. (2007) *Cell* **128,** 85–99
46. Radichev, I., Kwon, S. W., Zhao, Y., DePamphilis, M. L., and Vassilev, A. (2006) *J. Biol. Chem.* **281,** 23264–23273
47. Makise, M., Matsui, N., Yamairi, F., Takahashi, N., Takehara, M., Asano, T., and Mizushima, T. (2008) *J. Biochem.* **143,** 455–465
48. Branzei, D., and Foiani, M. (2006) *Exp. Cell Res.* **312,** 2654–2659
49. Shimada, K., Pasero, P., and Gasser, S. M. (2002) *Genes Dev.* **16,** 3236–3252
50. Gibson, D. G., Bell, S. P., and Aparicio, O. M. (2006) *Genes Cells* **11,** 557–573
51. Garber, P. M., and Rine, J. (2002) *Genetics* **161,** 521–534
52. Watanabe, K., Morishita, J., Umezu, K., Shirahige, K., and Maki, H. (2002) *Eukaryot. Cell* **1,** 200–212
53. Marahrens, Y., and Stillman, B. (1992) *Science* **255,** 817–823
54. Rao, H., and Stillman, B. (1995) *Proc. Natl. Acad. Sci. U. S. A.* **92,** 2224–2228
55. Semple, J. W., Da-Silva, L. F., Jervis, E. J., Ah-Kee, J., Al-Attar, H., Kummer, L., Heikkila, J. J., Pasero, P., and Duncker, B. P. (2006) *EMBO J.* **25,** 5150–5158
56. Asano, T., Makise, M., Takehara, M., and Mizushima, T. (2007) *FEMS Yeast Res.* **7,** 1256–1262
57. Harvey, S. L., and Kellogg, D. R. (2003) *Curr. Biol.* **13,** 264–275

50

THE JOURNAL OF BIOLOGICAL CHEMISTRY VOL. 284, NO. 7, pp. 4158–4167, February 13, 2009

Up-regulation of S100P Expression by Non-steroidal Anti-inflammatory Drugs and Its Role in Anti-tumorigenic Effects*

Received for publication, August 5, 2008, and in revised form, November 26, 2008 Published, JBC Papers in Press, December 10, 2008, DOI 10.1074/jbc.M806051200

Takushi Namba, Takashi Homan, Tomoko Nishimura, Shinji Mima, Tatsuya Hoshino, and Tohru Mizushima[1]

From the Graduate School of Medical and Pharmaceutical Sciences, Kumamoto University, Kumamoto 862-0973, Japan

Epidemiological studies have revealed that prolonged use of non-steroidal anti-inflammatory drugs (NSAIDs) reduces the risk of cancer. Various mechanisms, including induction of apoptosis and inhibition of the growth and invasion of cancer cells, have been implicated in this anti-tumorigenic activity. In this study we focused on S100P, which is known to be overexpressed in clinically isolated tumors and which functions through both intracellular and extracellular mechanisms. We showed the up-regulation of S100P expression in human gastric carcinoma cells treated with various NSAIDs, including celecoxib. The celecoxib-mediated up-regulation of S100P was suppressed by the transfection of cells with small interfering RNA for activating transcription factor 4 (ATF4), a transcription factor involved in the endoplasmic reticulum stress response. Furthermore, deletion of ATF4 binding consensus sequence located in the promoter of the *S100P* gene resulted in inhibition of celecoxib-mediated transcriptional activation of the gene. These results suggest that celecoxib up-regulates the expression of S100P through an ATF4-mediated endoplasmic reticulum stress response. Celecoxib inhibited the growth and induced apoptosis, and these actions could be either suppressed or stimulated by transfection of cells with S100P overexpression plasmid or small interfering RNA, respectively. Celecoxib also inhibited the invasive activity of the cells. Cromolyn, which inhibits the binding of S100P to its receptor, enhanced the celecoxib-mediated inhibition of cell invasion and growth but did not affect apoptosis. These results suggest that S100P affects apoptosis, cell growth, and invasion through either an intracellular or an extracellular mechanism and that the up-regulation of S100P expression by NSAIDs reduces their anti-tumorigenic activity.

Non-steroidal anti-inflammatory drugs (NSAIDs)[2] comprise a useful family of therapeutics. In addition to their anti-inflammatory effects, recent epidemiological studies have revealed that prolonged NSAID use reduces the risk of cancer, whereas preclinical and clinical studies have indicated that some NSAIDs, in particular celecoxib, are effective in the treatment and prevention of cancer (1). The anti-tumorigenic activity of NSAIDs is believed to involve various mechanisms, including induction of apoptosis, cell growth suppression, inhibition of angiogenesis, and inhibition of metastasis (cell invasion suppression) (2, 3).

NSAIDs act as inhibitors of cyclooxygenase (COX), an enzyme essential for the synthesis of prostaglandins (PGs). PGs, such as PGE_2, inhibit apoptosis of cancer cells and stimulate their growth and invasion as well as promote angiogenesis (4–6). Thus, it is certain that the anti-tumorigenic effect of NSAIDs was mediated mainly through the inhibition of COX. However, several lines of evidence now suggest that a COX-independent mechanism may also be involved (7, 8). To investigate this COX-independent mechanism, we used DNA microarray techniques to systematically search for genes in human gastric carcinoma (AGS) cells whose expression was altered by the NSAID indomethacin in a COX-independent manner (9, 10). This analysis revealed that NSAIDs induce an endoplasmic reticulum (ER) stress response (11). ER stress response is induced through transcription factors, such as activating transcription factor 6 (ATF6) 6 and ATF4 (12–14), and we have previously reported that both ATF4 and ATF6 are activated by various NSAIDs, including indomethacin and celecoxib (15, 16). In this study we focused our attention on S100P, the expression of which appears to be induced by indomethacin based on results from DNA microarray analysis (10).

S100P is a member of the S100 family of EF-hand Ca^{2+}-binding proteins (17). Overexpression of S100P has been observed in tumors clinically isolated from various tissue types, with the extent of the overexpression being positively correlated to the degree of malignancy (18–23). Overproduction of S100P appears to stimulate tumor malignancy through both intracellular and extracellular mechanisms (24). Secreted S100P binds to its receptor, the receptor for activated glycation end products (RAGE), thereby stimulating the invasion and

* This work was supported by grants-in-aid for Scientific Research from the Ministry of Health, Labor, and Welfare of Japan, grants-in-aid from Scientific Research from the Ministry of Education, Culture, Sports, Science, and Technology of Japan, and grants-in-aid from the Japan Science and Technology Agency. The costs of publication of this article were defrayed in part by the payment of page charges. This article must therefore be hereby marked "*advertisement*" in accordance with 18 U.S.C. Section 1734 solely to indicate this fact.

[1] To whom correspondence should be addressed: Graduate School of Medical and Pharmaceutical Sciences, Kumamoto University, 5-1 Oe-honmachi, Kumamoto 862-0973, Japan. Tel. and Fax: 81-96-371-4323; E-mail: mizu@gpo.kumamoto-u.ac.jp.

[2] The abbreviations used are: NSAID, non-steroidal anti-inflammatory drug; AARE, amino acid responsible element; ATF, activating transcription factor; BAPTA-AM, 1,2-bis(2-aminophenoxy)ethane-*N*,*N*,*N*′*N*′-tetraacetic acid; CHOP, C/EBP homologous transcription factor; COX, cyclooxygenase; ER, endoplasmic reticulum; ERK, extracellular-regulated kinase; GRP, glucose-regulated protein; MMP, matrix metalloproteinase; NF-κB, nuclear factor-κB; PG, prostaglandin; RAGE, receptor for activated glycation end products; siRNA, small interfering RNA; TPCK, *N*-*p*-tosyl-L-phenylalanine chloromethyl ketone; RT, reverse transcription.

growth of cancer cells or inhibiting their apoptosis through activation of extracellular-regulated kinase (ERK) and nuclear factor-κB (NF-κB) (20, 25–27). Furthermore, S100P was suggested to function also in cells through its binding to ezrin and Casy/SIP (28–30). It has recently been reported that S100P induces the expression of cathepsin D; however, the mechanism responsible for this effect is still to be identified (31).

It was recently reported that the expression of S100P is altered by some anti-tumor drugs (18, 32), although the underlying regulatory mechanism remains unknown. In this study we report that various NSAIDs up-regulate the expression of S100P through an ATF4-mediated ER stress response. Furthermore, our results suggest that up-regulation of S100P expression by NSAIDs negatively affects their anti-tumorigenic activity through inhibition of apoptosis, stimulation of cancer cell growth and invasion.

EXPERIMENTAL PROCEDURES

Materials and Animals—RPMI 1640 medium was obtained from Nissui Pharmaceutical Co. Fetal bovine serum was purchased from Invitrogen. 1,2-Bis(2-aminophenoxy)ethane-*N,N,N′N′*-tetraacetic acid (BAPTA-AM) was obtained from Dojindo Co. Cromolyn sodium salt, tunicamycin, normal mouse IgG, 1,4-diamino-2,3-dicyano-1,4-bis (*o*-aminophenylmercapto) butadiene ethanolate (U0126); *N-p*-tosyl-L-phenylalanine chloromethyl ketone (TPCK), and staurosporine were purchased from Sigma-Aldrich. Indomethacin, diclofenac, and thapsigargin were obtained from Wako Co. Celecoxib and meloxicam were from LKT Laboratories Inc. An antibody against actin, IκB, or RAGE was purchased from Santa Cruz Biotechnology Inc., antibody against ERK was from Cell Signaling, and antibody against S100P was from R&D Systems Inc. The RNeasy kit, siRNAs, HiPerFect, and RNAiFect were from Qiagen. A first-strand cDNA synthesis kit was purchased from Amersham Biosciences. Lipofectamine (TM2000), zymogram developing buffer, and pcDNA3.1 plasmid were obtained from Invitrogen. The iQ SYBR Green Supermix was from Bio-Rad. S100P enzyme-linked immunosorbent assay kits were purchased from CircuLex. Matrigel was from BD Biosciences, and the 24-well transwells were from Costar. The Dual Luciferase Assay System was from Promega. Male nonobese diabetes/severe combined immunodeficiency mice (5 weeks of age) were obtained from the Charles River. The experiments and procedures described here were carried out in accordance with the Guide for the Care and Use of Laboratory Animals as adopted and promulgated by the National Institute of Health and were approved by the Animal Care Committee of Kumamoto University.

Cell Culture and Overexpression of S100P—AGS, MKN45, and Kato III are human carcinoma cell lines derived from stomach. Cells were cultured in RPMI 1640 medium supplemented with 10% fetal bovine serum, 100 units/ml penicillin, and 100 μg/ml streptomycin in a humidified atmosphere of 95% air with 5% CO_2 at 37 °C. NSAIDs were dissolved in DMSO, and control experiments were performed in the same concentrations of DMSO alone. Cells were exposed to NSAIDs and other chemicals by changing the medium. Unless otherwise noted, cells were cultured for 24 h before use in experiments. The overexpression plasmid for S100P was constructed by insertion of S100P-encoding DNA fragments from the plasmid (S100P wild type (His tag), a gift from Dr. Gerke, University of Muenster (28)) into pcDNA3.1. Transfection of AGS cells with the plasmid was then carried out using Lipofectamine (TM2000) according to the manufacturer's protocols. Stable transfectants expressing S100P were selected by immunoblotting analysis. Positive clones were maintained in the presence of 800 μg/ml G418.

Real-time RT-PCR Analysis—Total RNA was extracted from cells using an RNeasy kit according to the manufacturer's instructions. Samples were reverse-transcribed using a first-strand cDNA synthesis kit. Synthesized cDNA was applied in real-time RT-PCR (Chromo 4 instrument (Bio-Rad)) experiments using iQ SYBR GREEN Supermix and analyzed with Opticon Monitor Software. The cycle conditions were 2 min at 50 °C followed by 10 min at 90 °C and finally 45 cycles each at 95 °C for 30 s and 63 °C for 60 s. Specificity was confirmed by electrophoretic analysis of the reaction products and by inclusion of template- or reverse transcriptase-free controls. To normalize the amount of total RNA present in each reaction, the actin gene was used as an internal standard. Primers were designed using the Primer3 Web site. Primers are listed as name, forward primer, and reverse primer: S100P, 5′-GATGCCGTGGATAAATTGCT-3′, 5′-ACTTGTGACAGGCAGACGTG-3′; cathepsin D, 5′-GACACAGGCACTTCCCTCAT-3′, 5′-CCTCCCAGCTTCAGTGTGAT-3′; actin, 5′-GGACTTCGAGCAAGAGATGG-3′, 5′-AGCACTGTGTTGGCGTACAG-3′.

Luciferase Assay—DNA fragments of the *S100P* promoter (from −1200 to −1) were amplified by PCR and ligated into the XhoI-HindIII site of the *Photinus pyralis* luciferase reporter plasmid, pGL3, to generate pS100Pluc. A plasmid with deletion of the amino acid-responsible element (AARE) sequence (33, 34) (from −84 to −76) was generated by PCR. All plasmids were sequenced to exclude unexpected mutations.

The luciferase assay was performed as described previously (11, 35). Cells were transfected with 1 μg of each of the *P. pyralis* luciferase reporter plasmids (pS100Pluc or its derivative) and 0.125 μg of the internal standard plasmid bearing the *Renilla reniformis* luciferase reporter (pRL-SV40). *P. pyralis* luciferase activity in cell extracts was measured using the Dual Luciferase Assay System and then normalized for *R. reniformis* luciferase activity.

Gelatin Zymography—The proteolytic activity of matrix metalloproteinase (MMP)-9 was assessed by SDS-PAGE using zymogram gels containing 0.1% (m/v) gelatin, as described previously (36). The culture medium was concentrated, and the protein concentration was determined according to the Bradford method (37). Following electrophoresis at 4 °C, the gels were washed with 2.5% Triton X-100 for 30 min at room temperature and incubated with zymogram development buffer for 2 days at 37 °C. Bands were visualized by staining with Coomassie Brilliant Blue.

Immunoblotting Analysis—Whole-cell extracts were prepared as described previously (38). The protein concentration of the samples was determined by the Bradford method (37). Samples were applied to polyacrylamide SDS gels and subjected

52

to electrophoresis, and the resultant proteins were then immunoblotted with their respective antibodies.

Analysis of Apoptosis by Fluorescence-activated Cell Sorting—Apoptosis was monitored by fluorescence-activated cell sorting analysis as described previously (39). Briefly, cells were collected by centrifugation. The pellets were fixed with 70% ethanol for 4 h at −20 °C, centrifuged, and re-suspended in phosphate-citrate buffer (0.2 M Na_2HPO_4 and 4 mM citric acid), then incubated for 20 min at room temperature. After centrifugation, the pellets were re-suspended in DNA staining solution (50 μg/ml propidium iodide and 10 μg/ml RNase A) and incubated for 20 min at room temperature. Samples were scanned with a FACSCalibur (BD Biosciences) cell sorter under conditions designed to measure only specific propidium iodide-mediated fluorescence. Apoptotic cells appeared as a hypodiploid peak due to nuclear fragmentation and loss of DNA.

Invasion Assay—The invasion assay was performed as previously described (40) with some modifications. Serum-free RPMI 1640 medium containing 5 mg/ml Matrigel was applied to the upper chamber of a 24-well transwell and incubated at 37 °C for 4 h. The cell suspension was applied to the Matrigel, and the lower chamber of the transwell was filled with culture medium containing 10% fetal bovine serum and 5 μg/ml fibronectin. The plate was incubated at 37 °C for 24 h. Cells were removed from the upper surface of the membrane, and the lower surface of the membrane was stained for 10 min with 0.5% crystal violet in 25% methanol, rinsed with distilled water, and air-dried overnight. The crystal violet was then extracted with 0.1 M sodium citrate in 50% ethanol, and the absorbance was measured at 585 nm.

siRNA Targeting of Genes—We used siRNA of 5′-GCCUAGGUCUCUUAGAUGAdTdT-3′ and 5′-UCAUCUAAGAGACCUAGGCdTdT-3′ or 5′-GCAACCAAUUAUCAGUUUAdTdT-3′ and 5′-UAAACUGAUAAUUGGUUGCdTdT-3′ as annealed oligonucleotides for repressing ATF4 or ATF6 expression, respectively. The siRNA for S100P was purchased from Qiagen. AGS cells were transfected with siRNA using RNAiFect or HiPerFect transfection reagents according to the manufacturer's instructions. Non-silencing siRNA (5′-UUCUCCGAACGUGUCACGUdTdT-3′ and 5′-ACGUGACACGUUCGGAGAAdTdT-3′) was used as a negative control.

Xenograft Tumor Growth—This assay was done as described (15, 16) with some modification. Briefly, each nonobese diabetes/severe combined immunodeficiency mouse was inoculated subcutaneously in the both flanks with 1×10^7 AGS cells. After 3 weeks, the mice began to receive a single daily intraperitoneal administration of cromolym, a protocol that continued for the duration of the study. Tumors were measured every 7 days, and their volumes were calculated.

Statistical Analysis—All values are expressed as the mean ± S.D. Two-way analysis of variance followed by the Tukey test or the Student's *t* test for unpaired results was used to evaluate differences between more than three groups or between two groups. Differences were considered to be significant for values of $p < 0.05$.

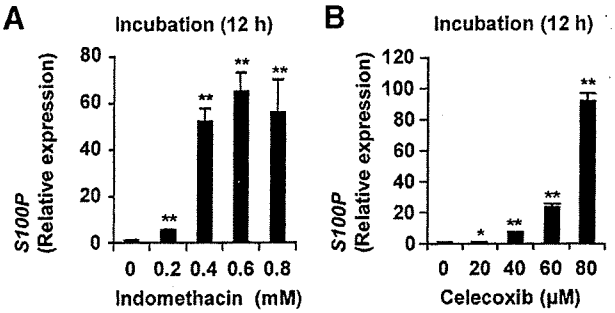

FIGURE 1. **Up-regulation of *S100P* mRNA expression by NSAIDs.** AGS cells were incubated with the indicated concentrations of indomethacin (*A*) or celecoxib (*B*) for the time periods indicated, and total RNA was extracted. Samples were subjected to real-time RT-PCR using a specific primer for *S100P*. Values were normalized to actin gene expression and expressed relative to the control sample (*i.e.* without NSAID). Values are given as the mean ± S.D. ($n = 3$). *, $p < 0.05$; **, $p < 0.01$.

RESULTS

NSAIDs Up-regulate S100P Expression—In a previous study we used DNA microarray analysis to search for genes whose expression is altered by indomethacin and found that *S100P* mRNA expression was up-regulated (10). In the present study we confirmed this result using a real-time RT-PCR technique. As shown in Fig. 1*A*, indomethacin up-regulated *S100P* mRNA expression in a dose-dependent manner. A similar result was obtained with the NSAID celecoxib, a finding that is particularly significant given its importance as an anti-cancer drug (Fig. 1*B*). Immunoblotting experiments revealed that celecoxib also up-regulates the expression of S100P at the protein level in both AGS cells and in another gastric cancer-derived cell line, MKN45 cells (Fig. 2, *A* and *E*). A similar response was observed in AGS cells with a number of other NSAIDs (indomethacin, meloxicam, and diclofenac; Fig. 2, *B*–*D*).

COX exists as two subtypes, COX-1 and COX-2. Given that celecoxib and meloxicam are COX-2 selective, the results shown in Fig. 2, *A*–*D*, suggest that NSAIDs up-regulate S100P expression irrespective of COX selectivity. We next examined the celecoxib-mediated up-regulation of S100P expression in Kato III cells, in which *COX-1* but not *COX-2* mRNA is expressed (41). This phenotype was confirmed by RT-PCR (data not shown). As shown in Fig. 2*F*, celecoxib up-regulated the expression of S100P even in the Kato III cells; in other words, a COX-2-selective NSAID up-regulated S100P expression in cells lacking COX-2 expression, suggesting that this occurs independently of COX inhibition. For further confirmation of this point, we examined the effect of PGE_2, revealing that it had no effect on the expression of S100P in the presence or absence of celecoxib (data not shown).

As described above, secreted S100P regulates various cell functions through its binding to RAGE (20, 25–28). We monitored the level of S100P in the culture medium by enzyme-linked immunosorbent assay and found that it increased in a dose-dependent manner in response to celecoxib treatment (Fig. 2*G*).

Mechanism for Up-regulation of S100P Expression by Celecoxib—As outlined above, the mechanism underlying the regulation of *S100P* expression is unknown. We have recently revealed that various NSAIDs including celecoxib induce an ER

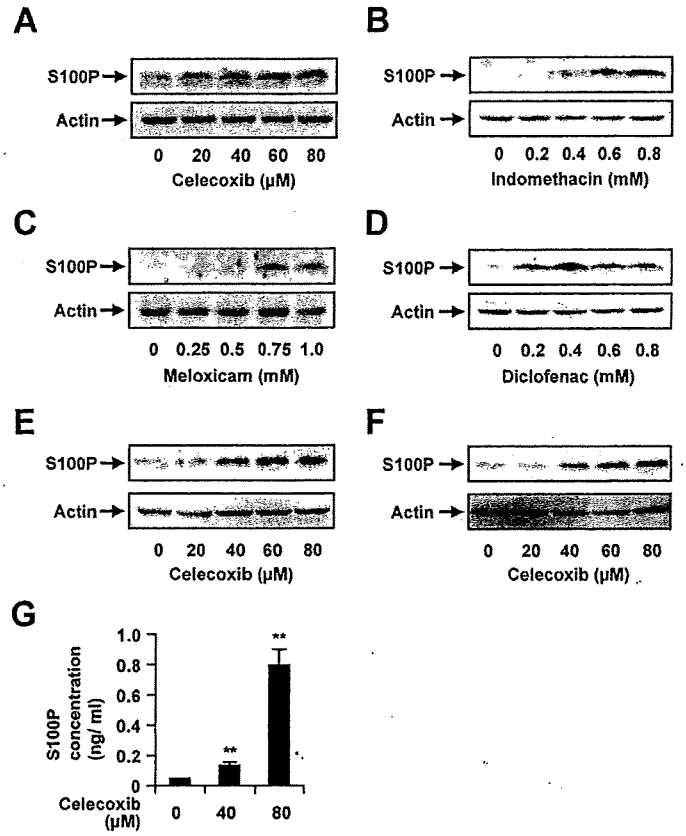

FIGURE 2. **Up-regulation of S100P expression by NSAIDs.** AGS (*A–D* and *G*), MKN-45 (*E*), or Kato III (*F*) cells were incubated with the indicated concentrations of NSAIDs for 12 h (*A* and *E–G*) or 24 h (*B–D*). Whole cell extracts were analyzed by immunoblotting with an antibody against S100P or actin (*A–F*). The level of S100P in the culture medium was determined by enzyme-linked immunosorbent assay. Values are given as the mean ± S.D. ($n = 3$). **, $p < 0.01$ (*G*).

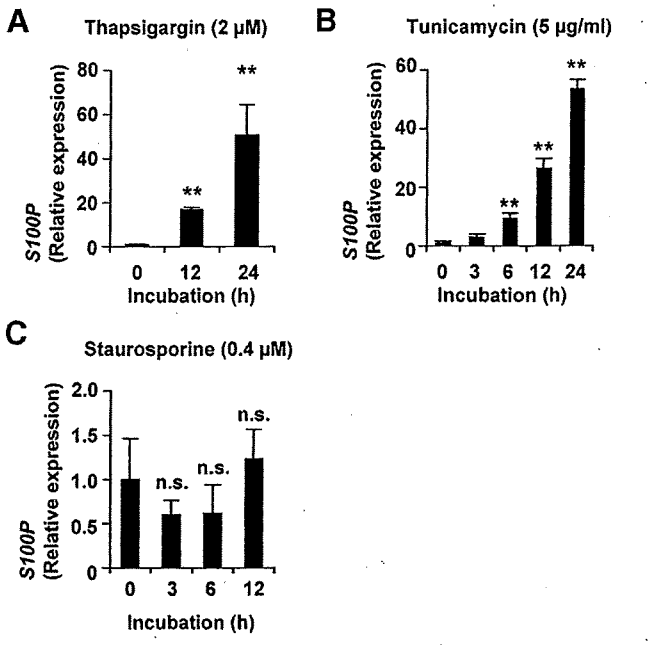

FIGURE 3. **Up-regulation of *S100P* mRNA expression associated with the ER stress response.** AGS cells were incubated with the indicated concentrations of thapsigargin (*A*), tunicamycin (*B*), or staurosporine (*C*) for the time periods indicated. *S100P* mRNA expression was monitored and expressed as described in the legend of Fig. 1. Values are given as mean ± S.D. ($n = 3$). **, $p < 0.01$; *n.s.*, not significant.

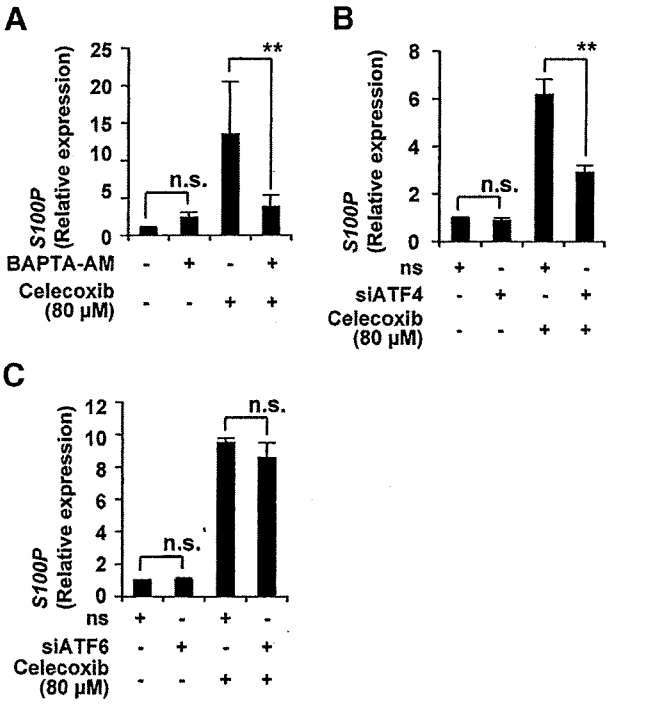

FIGURE 4. **Effect of siRNA for ATF4 or ATF6 on celecoxib-dependent up-regulation of *S100P* mRNA expression.** *A*, AGS cells were preincubated for 1 h with or without 2 μM BAPTA-AM, then incubated for a further 6 h with or without 80 μM celecoxib in the presence or absence of 2 μM BAPTA-AM. *B* and *C*, AGS cells were transfected with siRNA for ATF4 (*siATF4*), ATF6 (*siATF6*) or non-silencing siRNA (*n.s.*), with the total amount of siRNA fixed at 1 μg. After 24 h, the cells were treated with or without 80 μM celecoxib for 6 h. *S100P* mRNA expression was monitored and expressed as described in the legend of Fig. 1. Values are given as mean ± S.D. ($n = 3$). **, $p < 0.01$; *n.s.*, not significant.

stress response, and the concentration of each NSAID required to mediate this response (15) is similar to that which induces S100P expression (Fig. 2). We investigated the role of ER stress response in NSAID-induced S100P expression by examining the effect of other ER stress-inducing chemicals (thapsigargin and tunicamycin) on the expression of *S100P* mRNA. As shown in Fig. 3, *A* and *B*, both of these chemicals increased *S100P* mRNA. We also confirmed that both agents up-regulated the expression of glucose-regulated protein (GRP) 78 mRNA, a representative marker of the ER stress response at the concentration specified in Fig. 3, *A* and *B* (data not shown). In contrast, exposure to staurosporine, which does not produce such a response (15, 16), had no significant effect on *S100P* mRNA expression (Fig. 3*C*), suggesting that the expression of S100P is indeed linked to the ER stress response.

To confirm this we examined the effect of BAPTA-AM, an intracellular Ca^{2+} chelator, on celecoxib-mediated up-regulation of S100P. We have previously shown that NSAIDs increase the intracellular Ca^{2+} concentration and that this increase is required for the NSAID-induced ER stress response (15, 42). BAPTA-AM significantly inhibited the celecoxib-mediated up-regulation of *S100P* mRNA (Fig. 4*A*) and *GRP78* mRNA (data not shown) expression. At the concentration used, BAPTA-AM did not affect cell viability (data not shown). These results suggest that an increase in intracellular Ca^{2+} and the resultant induction of the ER stress response are somehow involved in the up-regulation of S100P. We next used siRNA for ATF4 and ATF6 to examine the contribution of these ER stress

54

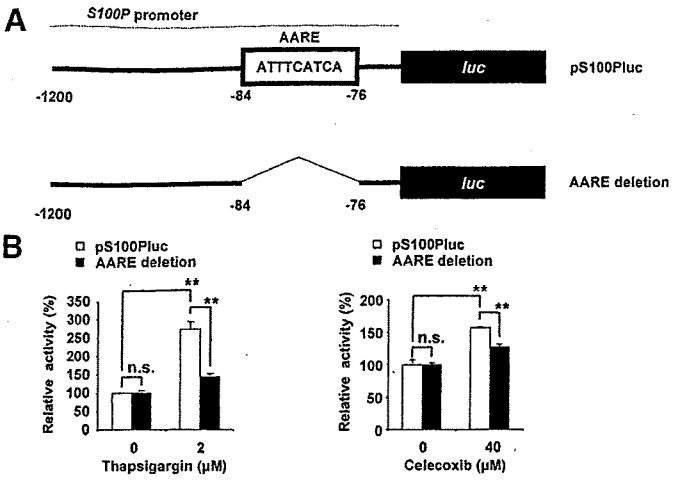

FIGURE 5. **ATF4-mediated activation of *S100P* gene promoter activity by celecoxib.** *A*, the structure of pS100Pluc and its AARE-deleted derivative (AARE deletion) is shown. *B*, AGS cells were co-transfected with pRL-SV40 (internal control plasmid carrying the *R. reniformis* luciferase gene) and pS100Pluc or its AARE-deleted derivative. After 24 h cells were treated with or without the indicated concentrations of thapsigargin or celecoxib for a further 24 h. *P. pyralis* luciferase activity was measured and normalized for *R. reniformis* luciferase activity. Values are the mean ± S.D. ($n = 3$). **, $p < 0.01$; *n.s.*, not significant.

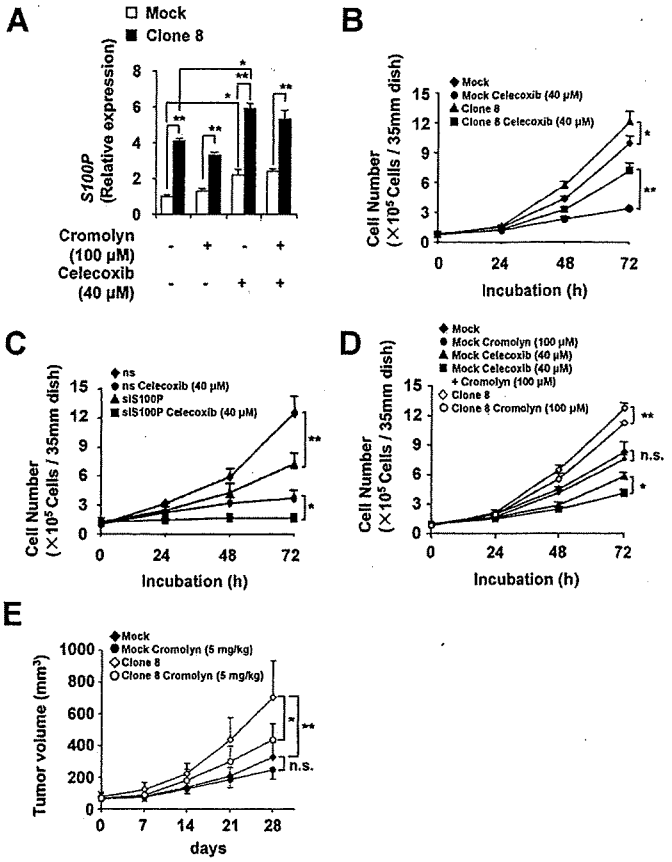

FIGURE 6. **Effect of S100P expression on celecoxib-dependent inhibition of cell growth.** S100P-overexpressing AGS cells (*Clone 8*) and mock transfectant-expressing control cells (*Mock*) were incubated with the indicated concentrations of celecoxib and/or cromolyn for either 24 h (*A*) or the indicated periods (*B* and *D*). *C*, AGS cells were transfected with siRNA for S100P (*siS100P*) or non-silencing siRNA (*ns*) with the total amount of siRNA fixed at 1 μg. After 24 h, cells were incubated with the indicated concentrations of celecoxib for the indicated periods. *A*, *S100P* mRNA expression was monitored and expressed as described in the legend of Fig. 1. *B–D*, cell numbers were determined by direct cell counting. Each mouse was inoculated with S100P-overexpressing AGS cells (*Clone 8*) and mock transfectant-expressing control cells (*Mock*), leading to tumor development. Cromolyn was then administered intraperitoneally as a single daily dose (5 mg/kg) for the duration of the study. Tumors were measured every 7 days, and their volumes are calculated (*E*). Values are the mean ± S.D. ($n = 3$ (*A–D*) or $n = 6$ (*E*)). *, $p < 0.05$; **, $p < 0.01$; *n.s.*, not significant.

response-related transcription factors to the celecoxib-dependent up-regulation of *S100P* mRNA expression. Transfection of a given siRNA decreased mRNA and protein levels of its target gene but had no effect on those of the other gene in either the absence or presence of celecoxib (data not shown). As illustrated in Fig. 4*B*, the transfection of siRNA for ATF4 suppressed the celecoxib-mediated up-regulation of *S100P* mRNA expression but did not affect its basal expression (Fig. 4*B*). In contrast, ATF6 siRNA had no significant effect on *S100P* mRNA expression (Fig. 4*C*), suggesting that ATF4 rather than ATF6 is responsible for the celecoxib-mediated transcriptional activation of the *S100P* gene.

AARE is the consensus sequence to which ATF4 binds when stimulating the transcription of downstream genes (33, 34). We identified the AARE sequence in the promoter of the *S100P* gene (Fig. 5*A*), then tested the contribution of this sequence to the celecoxib-mediated transcriptional activation of the gene by examining the effect of its deletion on the promoter activity of *S100P* gene using a reporter plasmid where the promoter of the *S100P* gene was inserted upstream of the luciferase gene (Fig. 5*A*). As shown in Fig. 5*B*, treatment of cells not only with celecoxib but also with thapsigargin stimulated the luciferase activity in the cells, suggesting that up-regulation of S100P expression by celecoxib is achieved at the level of transcription through the ER stress response. Furthermore, the deletion of AARE significantly decreased the luciferase activity in the presence of celecoxib or thapsigargin but not in their absence (Fig. 5*B*), indicating that ATF4 binding to AARE plays an important role in celecoxib-mediated transcriptional activation of the *S100P* gene.

Role of Up-regulation of S100P Expression in the in Vitro Anti-tumorigenic Activity of Celecoxib—As described above, various mechanisms have been proposed for the chemopreventive and chemotherapeutic action of NSAIDs; these include inhibition of cell growth and invasion and stimulation of apoptosis (2, 3). On the other hand, expression of S100P has been shown to stimulate the aggressiveness of cancer cells through stimulation of their growth and invasiveness and inhibition of apoptosis via both intracellular and extracellular mechanisms (20, 25–30). Here, we examined the role of celecoxib-mediated up-regulation of S100P expression in its anti-tumorigenic activity *in vitro*. This was achieved by constructing stable transfectants of AGS cells that continuously overexpressed S100P (Clone 8), this being confirmed at both the mRNA and protein levels (Fig. 6*A* and see Fig. 8*B*). Treatment of cells with celecoxib (40 μM) up-regulated the expression of *S100P* mRNA even in the S100P-overexpressing cells (Fig. 6*A*).

Fig. 6*B* shows the cell growth curve for S100P-overexpressing cells and mock transfectant control cells in the presence or absence of celecoxib; S100P-overexpressing cells had a faster growth rate than control cells in not only the absence but also the presence of celecoxib. We also examined the effect of S100P siRNA on celecoxib-mediated inhibition of cell growth after

first confirming that this siRNA, but not nonspecific siRNA, suppresses S100P expression at both the mRNA and protein levels (see Fig. 8, *E* and *F*). As shown in Fig. 6*C*, cell growth was significantly suppressed by S100P siRNA transfection in both the absence and the presence of celecoxib. These results suggest that celecoxib-mediated up-regulation of S100P expression weakens the inhibitory effect of the drug on AGS cell growth.

As described above, S100P functions extracellularly via its binding to RAGE (20, 25–27). To test the contribution of this extracellular mechanism, we examined the effect of cromolyn, an antiallergy drug that has recently been shown to act as an inhibitor of S100P binding to RAGE (27), on the celecoxib-mediated inhibition of cell growth. Cromolyn did not affect the expression of *S100P* mRNA (Fig. 6*A*). However, it slightly enhanced the inhibitory effect of celecoxib on cell growth without significantly affecting growth in the absence of the drug (Fig. 6*D*), suggesting that celecoxib-induced S100P may function extracellularly (via its binding to RAGE) to weaken the inhibitory effect of celecoxib on cell growth. In S100P-overexpressing cells, cromolyn slightly inhibited cell growth even in the absence of celecoxib, suggesting that the extracellular S100P signaling may generally (rather than specifically in the presence of celecoxib) play an important role in the regulation of cell growth.

We also examined the effect of overexpression of S100P and cromolyn on growth of xenograft tumors in immunodeficient nonobese diabetes/severe combined immunodeficiency mice characterized by T cell, B cell, and natural killer cell deficiency and lack of macrophage function. Tumors were developed in mice by inoculation subcutaneously of AGS cells (S100P-overexpressing (Clone 8) and mock transfectant control cells). Growth of xenograft tumors that overexpress S100P was faster than that of control (Fig. 6*E*). Intraperitoneal administration of cromolyn clearly inhibited the growth of xenograft tumors that overexpress S100P but not that of the control (Fig. 6*E*), suggesting that S100P stimulates the growth of AGS cells also *in vivo* extracellularly (via its binding to RAGE). Results are basically similar to those observed previously (27).

The invasive capacity of cancer cells is also important for the progression of tumors, especially in relation to metastasis, and we have recently reported that NSAIDs inhibit the invasiveness of AGS cells (9). Thus, we tested the contribution of up-regulation of S100P expression to celecoxib-mediated inhibition of cell invasiveness. As shown in Fig. 7*A*, celecoxib inhibited the invasive activity of AGS cells, an effect that was further stimulated in the presence of cromolyn. S100P-overexpressing cells displayed greater invasiveness than control cells in both the absence and the presence of celecoxib, with cromolyn reducing the invasive activity of the S100P-overexpressing cells but not that of control cells (Fig. 7*A*). Furthermore, even in the presence of celecoxib, S100P-overexpressing cells displayed greater invasiveness than control cells. We also examined the effect of neutralizing antibodies against S100P or RAGE on the S100P-overexpression-dependent stimulation of cell invasion activity. As shown in Fig. 7*B*, each neutralizing antibodies suppressed the S100P overexpression-dependent stimulation of cell invasion activity. All these results suggest that

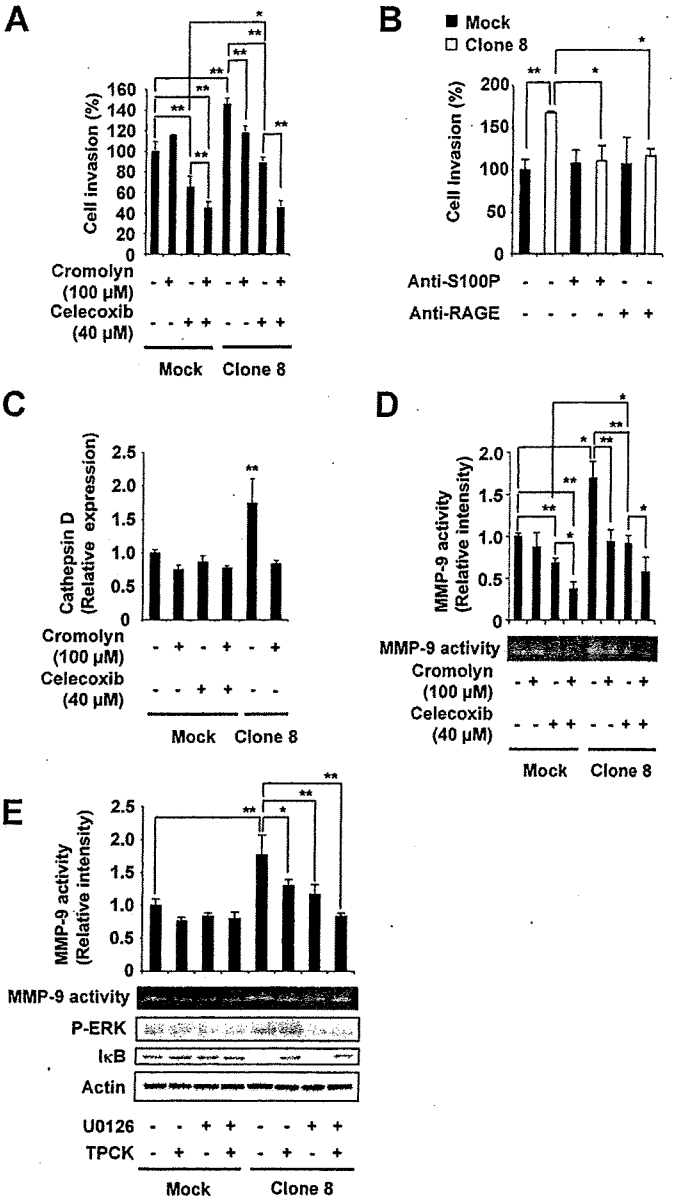

FIGURE 7. **Effect of S100P expression on celecoxib-dependent inhibition of cell invasion.** *A* and *B*, the invasive activity of S100P-overexpressing AGS cells (*Clone 8*) and mock transfectant control cells (*Mock*) was measured in the presence of the indicated concentrations of celecoxib and cromolyn or antibodies against S100P (20 μg/ml) or RAGE (2 μg/ml) as described under "Experimental Procedures" and is expressed relative to the control. *C* and *D*, S100P-overexpressing AGS cells (*Clone 8*) and mock transfectant-expressing control cells (*Mock*) were incubated with the indicated concentrations of celecoxib and/or cromolyn for 24 h. Both types of cells were preincubated with U0126 (20 μM) or TPCK (20 μM) for 1 h and further incubated for 24 h without the drug (*E*). The mRNA expression of cathepsin D was monitored and expressed as described in the legend of Fig. 1 (*C*). MMP-9 activity in the culture medium was measured as described under "Experimental Procedures." The clear band intensity was determined (*D* and *E*). The presence of phosphorylated ERK (*P-ERK*) and IκB was monitored by immunoblotting (*E*). Values are the mean ± S.D. ($n = 3$ (*A–C* and *E*) or 6 (*D*)). *, $p < 0.05$; **, $p < 0.01$; *n.s.*, not significant (*A–D*).

celecoxib-induced S100P decreases the inhibitory effect of the drug on cell invasion via its extracellular binding to RAGE.

It has recently been reported that S100P up-regulates the expression of cathepsin D, which stimulates the invasion of cancer cells (31). As shown in Fig. 7*C*, cathepsin D mRNA

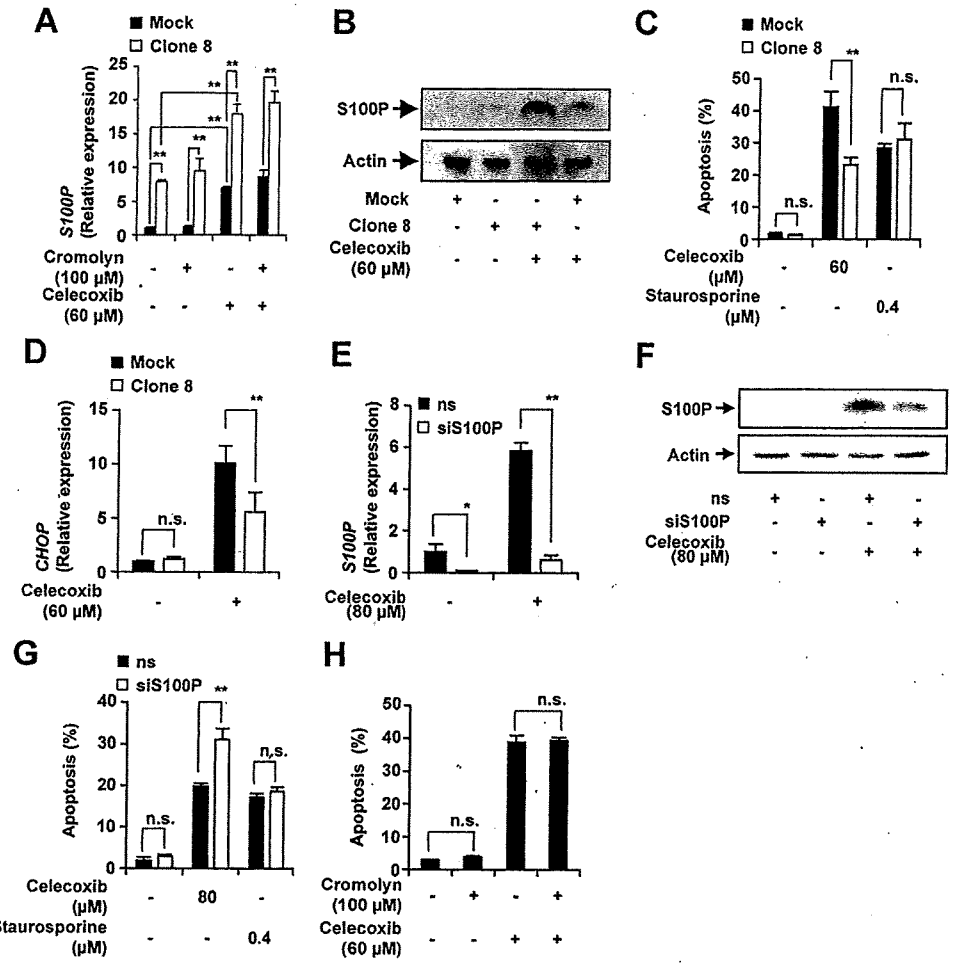

FIGURE 8. **Effect of S100P expression on celecoxib-induced apoptosis.** S100P-overexpressing AGS cells (*Clone 8*) and mock transfectant control cells (*Mock*) were incubated with the indicated concentrations of celecoxib, staurosporine, and/or cromolyn for 6 h (*A*), 12 h (*B*, *C*, and *H*) or 3 h (*D*). AGS cells were transfected with siRNA for S100P (*siS100P*) or non-silencing siRNA (*ns*), with the total amount of siRNA fixed at 1 μg. After 24 h the cells were incubated with the indicated concentrations of celecoxib or staurosporine for a further 6 h (*E*), 12 h (*F*), or 8 h (*G*). *S100P* or *CHOP* mRNA expression was monitored and expressed as described in the legend of Fig. 1 (*A*, *D*, and *E*). S100P expression was monitored as described in the legend of Fig. 2 (*B* and *F*). Apoptosis was determined by fluorescence activated cell sorting, as described under "Experimental Procedures" (*C*, *G*, and *H*). Values are the mean ± S.D. ($n = 3$). *, $p < 0.05$; **, $p < 0.01$; *n.s.*, not significant.

expression was higher in S100P-overexpressing cells than in control cells, an effect that was suppressed in the presence of cromolyn, suggesting that S100P up-regulates the expression of cathepsin D through the extracellular mechanism. However, celecoxib and/or cromolyn had no effect on cathepsin D mRNA expression in control cells (Fig. 7*C*). Therefore, expression of cathepsin D does not seem to be involved in the inhibitory effect of S100P on celecoxib-mediated suppression of cell invasiveness. MMPs, especially MMP-9, also play an important role in cell invasion (43, 44). We, therefore, next examined the effect of celecoxib and/or cromolyn on MMP-9 activity using gelatin zymography. The band intensity, indicative of MMP-9 activity, was decreased by treatment of cells with celecoxib, and this effect was further stimulated in the presence of cromolyn (Fig. 7*D*). S100P-overexpressing cells showed higher MMP-9 activity than control cells in both the presence and absence of celecoxib, and cromolyn inhibited MMP-9 activity in S100P-overexpressing cells (Fig. 7*D*). These results suggest that expression of S100P stimulates MMP-9 activity through the extracellular mechanism and that this mechanism is involved in the inhibitory effect of S100P on celecoxib-mediated suppression of cell invasion.

It was reported that S100P activates ERK and NF-κB (25, 26), both of which are known to activate MMP-9 (45–47), suggesting that the S100P-dependent activation of MMP-9 is mediated by ERK and NF-κB. To test this idea, we examined the effect of an inhibitor for ERK or NF-κB on S100P-dependent activation of MMP-9. We confirmed that overexpression of S100P caused phosphorylation (activation) of ERK and decrease in the amount of IκB (an inhibitor for NF-κB) (Fig. 7*E*), both of which were inhibited by cromolyn (data not shown). As shown in Fig. 7*E*, treatment of cells with U0126, an inhibitor of ERK phosphorylation (activation), inhibited not only S100P-dependent phosphorylation of ERK but also activation of MMP-9. Treatment of S100P-overexpressing cells with TPCK (an inhibitor of proteasome system that depredates IκB) recovered the level of IκB in S100P-overexpressing cells (Fig. 7*E*), suggesting that this agent inhibited the activity of NF-κB. Treatment of cells with TPCK inhibited S100P-dependent activation of MMP-9. Results in Fig. 7*E* suggest that the S100P-dependent activation of MMP-9 is mediated by ERK and NF-κB.

We have recently reported that celecoxib induces apoptosis through induction of the ER stress response, particularly the induction of CHOP (11, 15). Here we examined the role of up-regulation of S100P expression in apoptosis induced by celecoxib. Celecoxib at a concentration of 60 μM up-regulated the expression of both S100P mRNA and protein not only in control cells but also in S100P-overexpressing cells (Fig. 8, *A* and *B*). Treatment of AGS cells with celecoxib at the same concentration clearly induced apoptosis, as described above (16), and this apoptosis was significantly suppressed in S100P-overexpressing cells (Fig. 8*C*). Celecoxib-induced expression of *CHOP* mRNA was also suppressed in S100P-overexpressing cells (Fig. 8*D*). These results suggest that S100P induction inhibits celecoxib-induced apoptosis through suppression of CHOP expression. We further tested this idea using siRNA for S100P and an 80 μM concentration of celecoxib. Transfection of S100P siRNA decreased the expression of *S100P* mRNA (Fig. 8*E*) and S100P protein (Fig. 8*F*) in the presence or absence of celecoxib (80 μM). This transfection stimulated celecoxib-induced apoptosis but not its basal level (Fig. 8*G*).

57

To examine the specificity of this anti-apoptotic effect of S100P, the apoptosis induced by staurosporine was compared between S100P-overexpressing cells and the mock transfectant control cells. As shown in Fig. 8*C*, staurosporine-induced apoptosis was indistinguishable between S100P-overexpressing cells and control cells. Furthermore, transfection of S100P siRNA did not affect this outcome (Fig. 8*G*). These results suggest that the suppression of apoptosis by overexpression of S100P is specific for apoptosis induced by ER stress response-inducing drugs.

Finally, we also tested the contribution of the extracellular S100P signaling to its inhibitory effect on celecoxib-induced apoptosis using cromolyn. Cromolyn did not affect the expression of *S100P* mRNA in the presence or absence of celecoxib (Fig. 8*A*). As shown in Fig. 8*H*, treatment of cells with cromolyn had no effect on celecoxib-induced apoptosis, suggesting that extracellular mechanisms are not involved in the inhibitory effect of S100P in this situation.

DISCUSSION

In this study we have shown that various NSAIDs, including celecoxib, a drug that is clinically used for cancer therapy, up-regulate the expression of S100P in cultured cancer cells. Given that celecoxib (a COX-2 selective NSAID) up-regulated the expression of S100P in Kato III cells that lack *COX-2* mRNA expression and that exogenous application of PGE_2 did not affect this up-regulation, it appears to occur independent of COX inhibition, as does the up-regulation of GRP78 and oxygen-regulated protein 150 by the same drug (15, 16). S100P has previously been reported to be overexpressed in tumors clinically isolated from various tissue types, and expression of S100P has been shown to stimulate the aggressiveness of cancer cells (18–23, 25, 26, 28, 48, 49). Thus, up-regulation of S100P could play an important role in the anti-tumorigenic activity of NSAIDs (see below).

Although the expression of S100P in clinically isolated tumors has been well described, little is known about the effect of anti-tumor drugs on the expression of S100P. Only bifunctional alkylating agents and retinoic acid have been shown to up-regulate S100P expression, although the mechanism governing this up-regulation remains unknown (18, 32). Based on the following combination of results from this study, we strongly suggest that celecoxib up-regulates the expression of S100P through an ATF4-mediated ER stress response; celecoxib-dependent up-regulation of S100P expression was suppressed by siRNA for ATF4, other ER stress response-inducing chemicals (thapsigargin and tunicamycin) also up-regulated the expression of S100P, and deletion of the ATF4 binding consensus sequence (AARE) in the *S100P* gene promoter resulted in inhibition of celecoxib-dependent activation of its promoter activity. ER stressors phosphorylate protein kinase R-like ER kinase located in the ER membrane, which in turn phosphorylates eukaryotic initiation factor-2α, leading to induction of ATF4 expression (50). We have previously reported that celecoxib stimulates the phosphorylation of both protein kinase R-like ER kinase and eukaryotic initiation factor-2α and induces the expression of ATF4, all of which are inhibited in the presence of the intracellular Ca^{2+} chelator, BAPTA-AM (15). In this study we have shown that BAPTA-AM also inhibits the celecoxib-mediated up-regulation of S100P expression. We have also demonstrated that NSAIDs could cause permeabilization of cytoplasmic membranes, resulting in an increase in intracellular Ca^{2+} due to stimulation of the influx of extracellular Ca^{2+} (42, 51). Therefore, it seems that celecoxib up-regulates the expression of *S100P* mRNA through permeabilization of cytoplasmic membranes, an increase in the intracellular Ca^{2+} level, phosphorylation of both protein kinase R-like ER kinase and eukaryotic initiation factor-2α, and induction of ATF4 expression. As far as we are aware, this is the first indication of the mechanism underlying transcriptional regulation of S100P expression by anti-tumor drugs, information which should prove valuable in increasing our understanding of the modes of action of other anti-tumor drugs, and the role of S100P overexpression in tumors *in vivo*. For example, because it has been suggested that retinoic acid induces the ER stress response (52), retinoic acid may induce the expression of S100P via ER stress response.

It is well known that S100P stimulates the aggressiveness of cancer cells in various ways (including inhibition of apoptosis and stimulation of growth and invasion of cancer cells) and that NSAIDs, especially celecoxib, display their anti-tumor activity by exerting the opposite effects. Therefore, understanding the role of up-regulation of S100P expression in the anti-tumor activity of NSAIDs is important if we are to apply these drugs to cancer therapy. Here we have demonstrated that celecoxib-mediated inhibition of growth and invasion and induction of apoptosis are suppressed in S100P-overexpressing cells, and celecoxib-mediated inhibition of growth and induction of apoptosis were stimulated by transfection of cells with S100P siRNA. These results suggest that S100P induced by celecoxib decreases the anti-tumor activity of the drug. In the case of apoptosis, we have also shown that S100P suppresses the celecoxib-induced expression of CHOP, an ER stress-induced transcriptional factor with apoptosis-inducing ability. Furthermore, expression of S100P did not affect staurosporine-induced apoptosis. These findings suggest that S100P exerts a protective effect against accumulation of unfolded proteins in the ER, resulting in suppression of the ER stress response and apoptosis. Because some proteins of the S100 family have been reported to function as molecular chaperones, it is possible that S100P acts as ER chaperones to protect cells from ER stressors. We also found that expression of S100P activates MMP-9 activity and suppresses the inhibitory effect of celecoxib on this activity, suggesting that MMP-9 is involved in the effect of S100P on celecoxib-mediated inhibition of cell invasion. This is likely due to the fact that S100P activates ERK and NF-κB (25, 26), both of which are known to activate MMP-9 (45–47).

S100P functions through both intracellular (example, Ca^{2+}-dependent binding to ezrin) and extracellular (binding to RAGE and resulting activation of ERK and NF-κB) mechanisms. Here we used cromolyn to test which pathway is dominant for the inhibitory effect of S100P on the anti-tumorigenic potential of celecoxib. Cromolyn not only inhibited the growth and invasion of S100P-overexpressing cells (but not control cells) but also stimulated the celecoxib-mediated inhibition of cell growth and invasion, suggesting that celecoxib-induced